Impact of plasma-wall interaction and exhaust on the EU-DEMO design

Nuclear Materials and Energy 26 (2021) 100897

Contents lists available at ScienceDirect

Nuclear Materials and Energy

journal homepage: www.elsevier.com/locate/nme

Impact of plasma-wall interaction and exhaust on the EU-DEMO design

F. Maviglia [a,b], M. Siccinio [a,c,*], C. Bachmann [a], W. Biel [d], M. Cavedon [c], E. Fable [c], G. Federici [a], M. Firdaouss [e], J. Gerardin [f], V. Hauer [g], I. Ivanova-Stanik [h], F. Janky [c], R. Kembleton [a,i], F. Militello [i], F. Subba [l], S. Varoutis [g], C. Vorpahl [a,g]

[a] EUROFusion Consortium, Garching bei München, Germany
[b] Associazione EURATOM-ENEA, Frascati, Rome, Italy
[c] Max-Planck-Institut für Plasmaphysik, Garching bei München, Germany
[d] Forschungszentrum Jülich, Jülich, Germany
[e] CEA, Cadarache, France
[f] Institute of Plasma Physics, Prague, Czech Republic
[g] Karlsruhe Institut für Technologie (KIT), Karlsruhe, Germany
[h] Institute of Plasma Physics and Laser Microfusion, Warsaw, Poland
[i] Culham Centre for Fusion Energy, Abingdon, United Kingdom
[l] NEMO Group, Politecnico di Torino, Turin, Italy

ARTICLE INFO

Keywords:
EU-DEMO
Limiters
Disruptions
Divertor reattachment
ELMs
Transients

ABSTRACT

In the present work, the role of plasma facing components protection in driving the EU-DEMO design will be reviewed, focusing on steady-state and, especially, on transients. This work encompasses both the first wall (FW) as well as the divertor. In fact, while the ITER divertor heat removal technology has been adopted, the ITER FW concept has been shown in the past years to be inadequate for EU-DEMO. This is due to the higher foreseen irradiation damage level, which requires structural materials (like Eurofer) able to withstand more than 5 dpa of neutron damage. This solution, however, limits the tolerable steady-state heat flux to ~1 MW/m^2, i.e. a factor 3–4 below the ITER specifications. For this reason, poloidally and toroidally discontinuous protection limiters are implemented in EU-DEMO. Their role consists in reducing the heat load on the FW due to charged particles, during steady state and, more importantly, during planned and off-normal plasma transients. Concerning the divertor configuration, EU-DEMO currently assumes an ITER-like, lower single null (LSN) divertor, with seeded impurities for the dissipation of the power. However, this concept has been shown by numerous simulations in the past years to be marginal during steady-state (where a detached divertor is necessary to maintain the heat flux below the technological limit and to avoid excessive erosion) and unable to withstand some relevant transients, such as large ELMs and accidental loss of detachment. Various concepts, deviating from the ITER design, are currently under investigation to mitigate such risks, for example in-vessel coils for strike point sweeping in case of reattachment, as well as alternative divertor configurations. Finally, a broader discussion on the impact of divertor protection on the overall machine design is presented.

1. Introduction

The European (EU) DEMO is mentioned in the EU-Roadmap [1] as the first device able to reliably demonstrate a net electricity production of few hundred MW, breed its fusion fuel (tritium) and exhibit a sufficiently high availability, thus a long lifetime of its components. The main purpose of EU-DEMO is in fact to show the ability of successive, commercial Fusion Power Plants (FPP) to play a role in the energy market.

The approach to the design and realisation of EU-DEMO consists of assuming the ITER baseline as the starting point for the plant definition, and in general taking advantage as much as possible of the ITER experience [2]. However, there are aspects for which the ITER solution is not applicable to DEMO, either because of physics and technology non-linearities which prevent simple extrapolations, or because of the different missions the two devices have to accomplish.

First-wall protection is a clear example of this occurrence. ITER can in fact afford a robust first-wall, able to withstand high power density

* Corresponding author.
E-mail address: mattia.siccinio@euro-fusion.org (M. Siccinio).

https://doi.org/10.1016/j.nme.2020.100897
Received 31 July 2020; Received in revised form 16 December 2020; Accepted 30 December 2020
Available online 8 January 2021

during stationary phases (up to 5 MW/m^2) [3] and able to tolerate a certain number of unplanned plasma-wall contacts at high current before being irreversibly damaged. The situation looks different in DEMO. The higher neutron fluence on the plasma facing components, due to both a higher fusion power and a longer required lifetime, has forced the designers to adopt materials, like Eurofer, able to survive in such a challenging environment [4,5]. Eurofer however cannot tolerate heat fluxes of the order of the ITER ones, and thus a reduction of the maximum allowable power density of a factor 3–4 is necessary. In addition, the thickness of the first wall is appreciably less than the ITER one, since DEMO has to allow for T breeding, which requires the neutrons to be able to stream across the Plasma Facing Components (PFC) and to then be absorbed in the breeding region. This "weakness" of the EU-DEMO wall requires that, essentially, no plasma-wall contact can happen, especially at plasma currents close to the nominal flat-top value. For these reasons, high heat flux "sacrificial" limiters are foreseen in the DEMO design [6,7,8]. Their role in the various phases of the plasma discharge, as well as the thermal fluxes they are supposed to encounter, is discussed in great detail in the next sections.

Concerning the divertor, EU-DEMO currently foresees an ITER-like lower single null (LSN) configuration - although other configurations are under investigations and may enter the baseline in the next years [9,10]. Thus, at least from a qualitative point of view, the impact of the heat exhaust management during the steady-state phase does not particularly affect the reactor outlook, since the ITER solution has been adopted. There are however discrepancies on the strategies to manage unplanned transients, e.g. divertor reattachment, thus leading indeed to modifications in the plant design [11]. This is discussed in detail in the main text.

This paper is structured as follows: in section 2, a brief overview on the EU-DEMO machine parameters is provided. In section 3, the main phenomena driving the design of the first-wall, both during steady-states and transients, are discussed, with special emphasis on the protection limiters. Section 4 concerns the divertor main design drivers, again analysing both steady states and transients, finally providing an evaluation on the impact of the divertor protection on the machine design on a more general level. Section 5 contains a brief discussion on Edge Localised Modes (ELMs), whereas conclusions are drawn thereafter.

2. EU-DEMO parameters

The EU-DEMO project just concluded its so-called pre-conceptual design phase [2]. For the time being, no final decision has been taken on the parameters of the machine, but only a provisional design exists. In Table 1 below, the most relevant physics parameters referring to the latest H-mode baseline, released in spring 2018 and produced by the systems code PROCESS [12,13] are shown.

Table 1 is taken from [14]. The corresponding values of the considered quantities for of ITER 15 MA baseline scenario [15,16] are also reported for comparison. As mentioned in the introduction, the reference EU-DEMO scenario is analogous to the ITER 15 MA baseline, both assuming a pulsed operation in ELMy H-mode [17] with a confinement time in line with the well-known IPB98(y,2) scaling [18]. The interested reader is referred to [14] for further details.

Contrary to ITER, the entire PFC in EU-DEMO are coated with tungsten. This includes the divertor, the wall covering the breeding region and the protection limiters discussed below.

3. First wall protection

3.1. Steady state

In general, there are three typologies of heat load which the plasma deposits on the PFC: power carried by electromagnetic radiation, power carried by charged particles and power carried by neutrals. It is here incidentally noted that the neutron absorption is rather a volumetric process than a surface process, thus not directly impacting on the PFC design. Neutron heat load deposition is not subject of the present paper, the interested reader is referred, for example, to [19,20,21].

Table 1
EU-DEMO Physics Baseline 2018 relevant machine parameters and corresponding values for ITER. EU-DEMO data have been produced with the systems code PROCESS. The table is taken from [14].

	EU-DEMO 2018	ITER
R[m]	9.00	6.2
A	3.1	3.1
B_0[T]	5.86	5.3
q_{95}	3.89	3
δ_{95}	0.33	0.33
κ_{95}	1.65	1.7
I_p[MA]	17.75	15
f_{NI}	0.39	~0.2
f_{CD}	<5%	5–10%
P_{fus}[MW]	2000	500
P_{sep}[MW]	170.4	89
P_{LH}[MW]	120.8	52
H_{98}	0.98	1
$< n > /n_{GW}$	1.2	~1
$< T >$[keV]	12.49	8.9
β_N[% mT/MA]	2.5	1.8
Z_{eff}	2.12	1.78
$P_{sep}B/q_{95}AR$[MW T /m]	9.2	8.2
P_{sep}/R[MW/m]	18.9	14.35
Pulse length [sec]	7200	600

3.1.1. Radiation

One important point with respect to which ITER and EU-DEMO differ is the large amount of core radiation, which is necessary in EU-DEMO to protect the divertor by keeping P_{sep} reasonably close to P_{LH}, but not substantially above it [14,22]. In ITER, the unavoidable synchrotron and bremsstrahlung losses reduce the power carried by charged particles across the separatrix from the 150 MW of heating power P_{heat} (corresponding to 100 MW α's plus 50 MW P_{aux}) to about 80 MW, which can be dealt with by the divertor in presence of seeded SOL impurities, e.g. Ne or N [23]. The situation is however different in EU-DEMO, where, in absence of additional core radiation, the power P_{sep} would be larger than 350 MW, an amount which could not be radiated in the SOL and divertor volume without compromising the stability of the discharge. Thus, an high-Z impurity, e.g. Xe [22], is seeded in the EU-DEMO core (on top of the SOL seeded radiator, which is Ar), with the purpose of enhancing the overall fraction of power exhausted via radiation, which uniformly distributes on the very large first wall surface and does not concentrate on the small target wetted area.

The energy flows for the two devices are depicted in Fig. 1. The differences between P_{heat} and P_{sep}, and between P_{sep} and P_{target}, correspond to the core and SOL radiation amount, respectively. In the EU-DEMO group, kinetic profiles for the core region are typically evaluated with the 1.5D code ASTRA [24,25,26], and this encompasses also the radiation source profiles for the core (where "radiation" includes all sources, namely synchrotron, bremsstrahlung and line radiation). The ASTRA calculations have been performed determining the transport coefficients with TGLF. Xe has been added until $P_{sep} = 1.2P_{LH}$, while the pedestal width is assumed to be 5% of the minor radius (i.e. about 15 cm). Pedestal top density has been set to $0.85n_{GW}$, while safety factor, plasma elongation and triangularity, as well as toroidal magnetic field, are input parameters. The resulting plasma profiles have been plotted in [14]. Xe density has furthermore been assumed to be constant along the radius, which corresponds to a decreasing concentration from the edge to the centre.

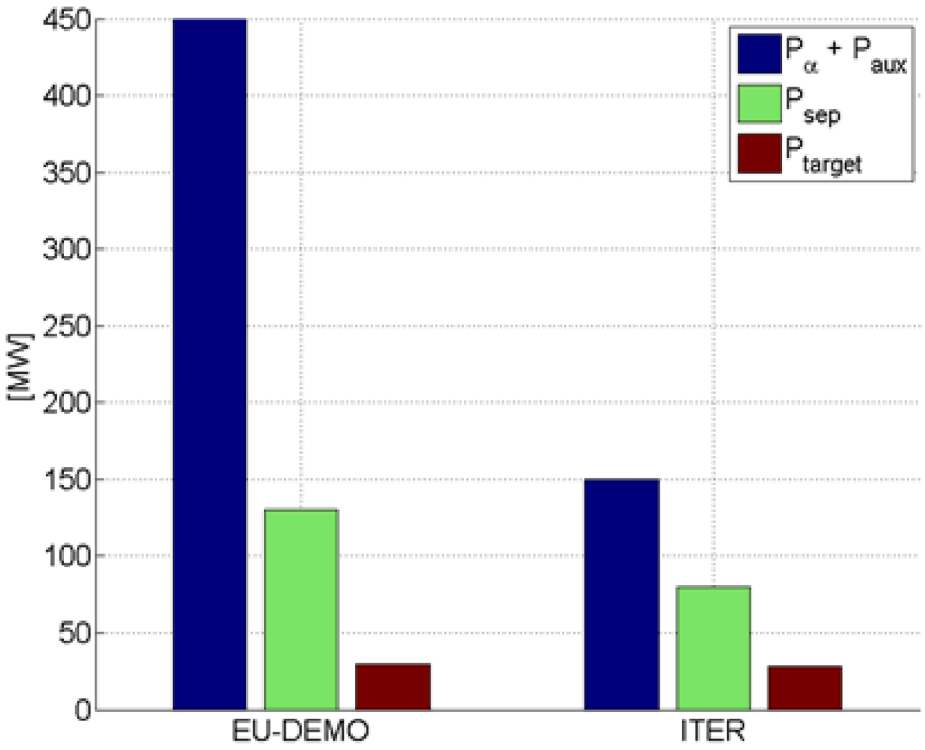

Fig. 1. Total heating power, power at the separatrix and maximum tolerable divertor power in ITER and EU-DEMO. Figure is taken from [14].

On the contrary, the SOL radiation profiles (again including all source terms) can be read in the dedicated SOLPS runs (see e.g. [27,28]). Superposing the results of the two codes, a 2D radiation source map can be produced, as shown in Fig. 2. This can be in turn used as an input to evaluate the impacting radiation on the FW and divertor during steady state phases. Note that, at the moment, there is no perfect overlap between the ASTRA and SOLPS computational domains. It is however assumed that, for a given total radiative power level, the spatial distribution in the core region (which is not expected to possess a strong dependence on the poloidal coordinate) does not exhibit a strong impact on the final result, also because the peak radiation level which is found (see in the following) is sufficiently below the technological limit to accept these uncertainties. More detailed calculations are in any case foreseen in the near future.

It is important here to stress once more that the first wall in a machine like the EU-DEMO is much thinner than in ITER because of the need to breed tritium. In fact, the ITER FW concept has been shown in the past years to be inadequate for EU-DEMO. This is due to the higher foreseen irradiation damage level, which requires structural materials (like Eurofer) able to withstand more than 5 dpa of neutron damage. This solution, however, limits the tolerable steady-state heat flux to ~ 1 MW/m^2, i.e. a factor 3–4 below the ITER specifications There is in fact only a ~ 3 mm metal layer between the plasma chamber and the high pressure coolant [4,5].

The heat flux on FW corresponding to (core and SOL) radiation is evaluated with the code CHERAB, which is a Monte Carlo ray tracing code [29,30] able to determine the power deposition profile on 3D surfaces (although the plasma source is always assumed to be toroidally symmetric). Results corresponding to the source above are shown in Figs. 3, 4 and 5.

As one can observe, following conclusions can be drawn:

- The highest flux from electromagnetic radiation is localised on the divertor plates, where it reaches values close to 2 MW/m^2. This is however not critical, since the divertor, as discussed in the next sections, can withstand up to 10 MW/m^2 [31] (there is no breeding

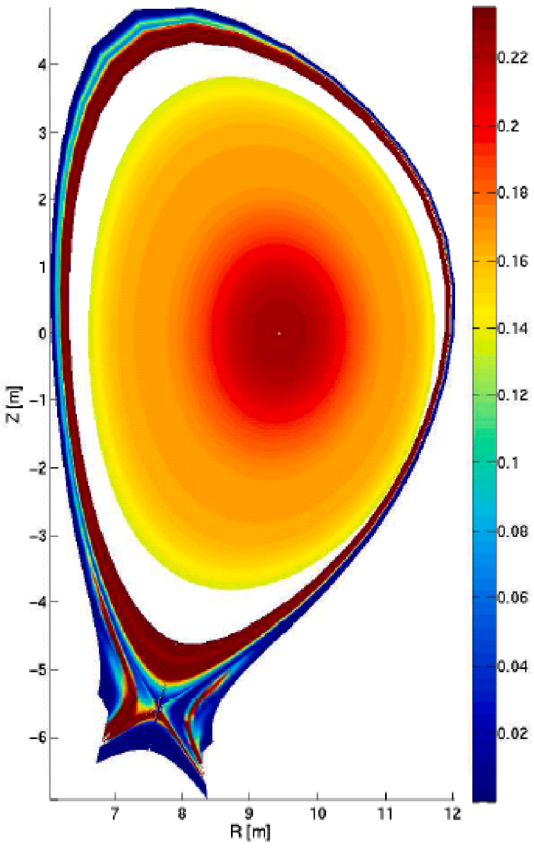

Fig. 2. 2D radiation density map for EU-DEMO flat-top – units are MW/m^3. The core values have been calculated with ASTRA, the SOL values are taken from a SOLPS detached case with fluid neutrals. The impact of the non-perfect matching of the two contributions is discussed in the main text.

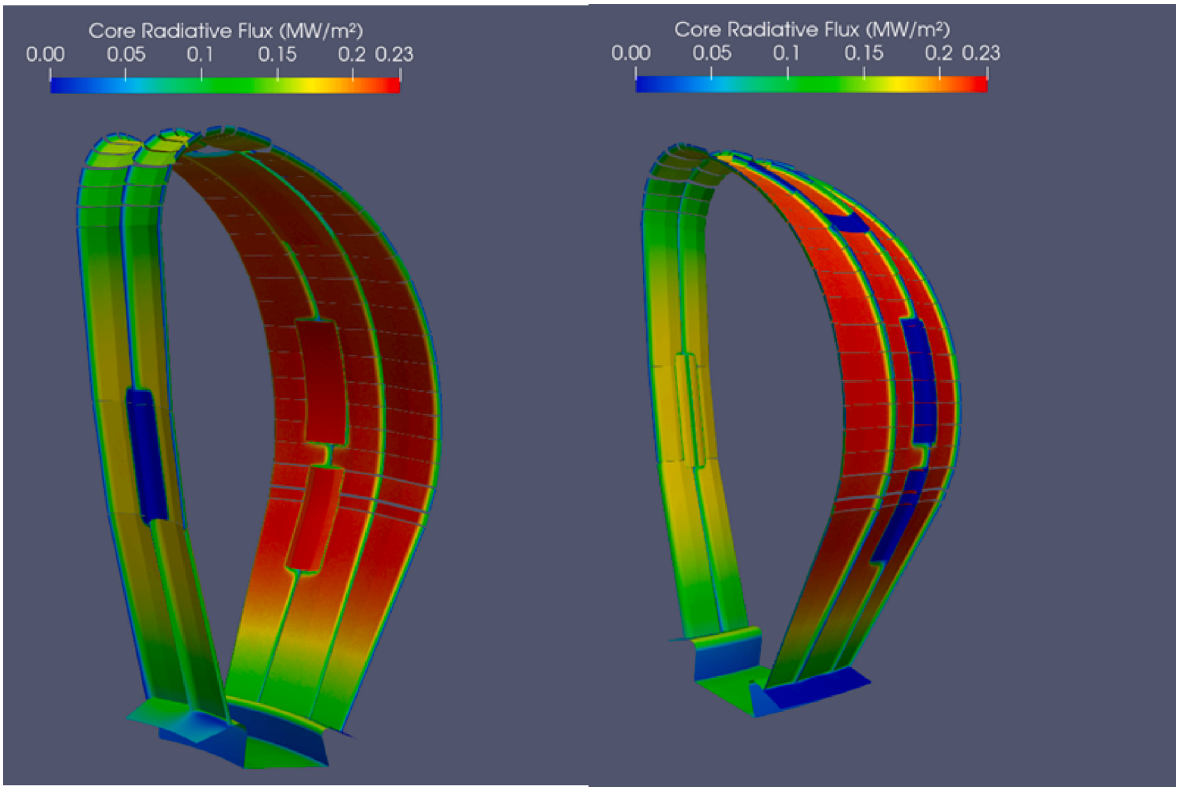

Fig. 3. Heating power distribution on the FW of a EU-DEMO sector when considering only the core source calculated with ASTRA.

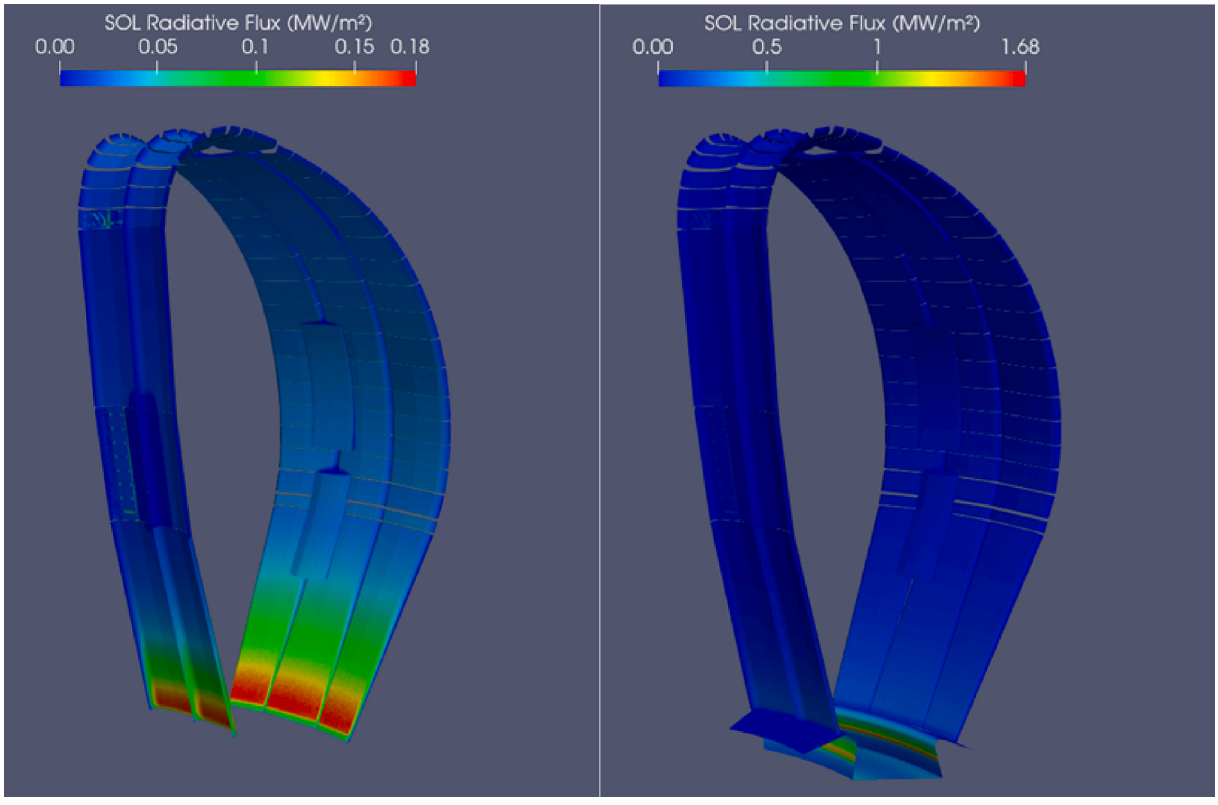

Fig. 4. Heating power distribution on the FW of a EU-DEMO sector when considering only the SOL core source calculated with SOLPS. The figure on the left does not depict the divertor region in order to allow a focus on the FW blanket modules (note also the different colour scale among the two figures).

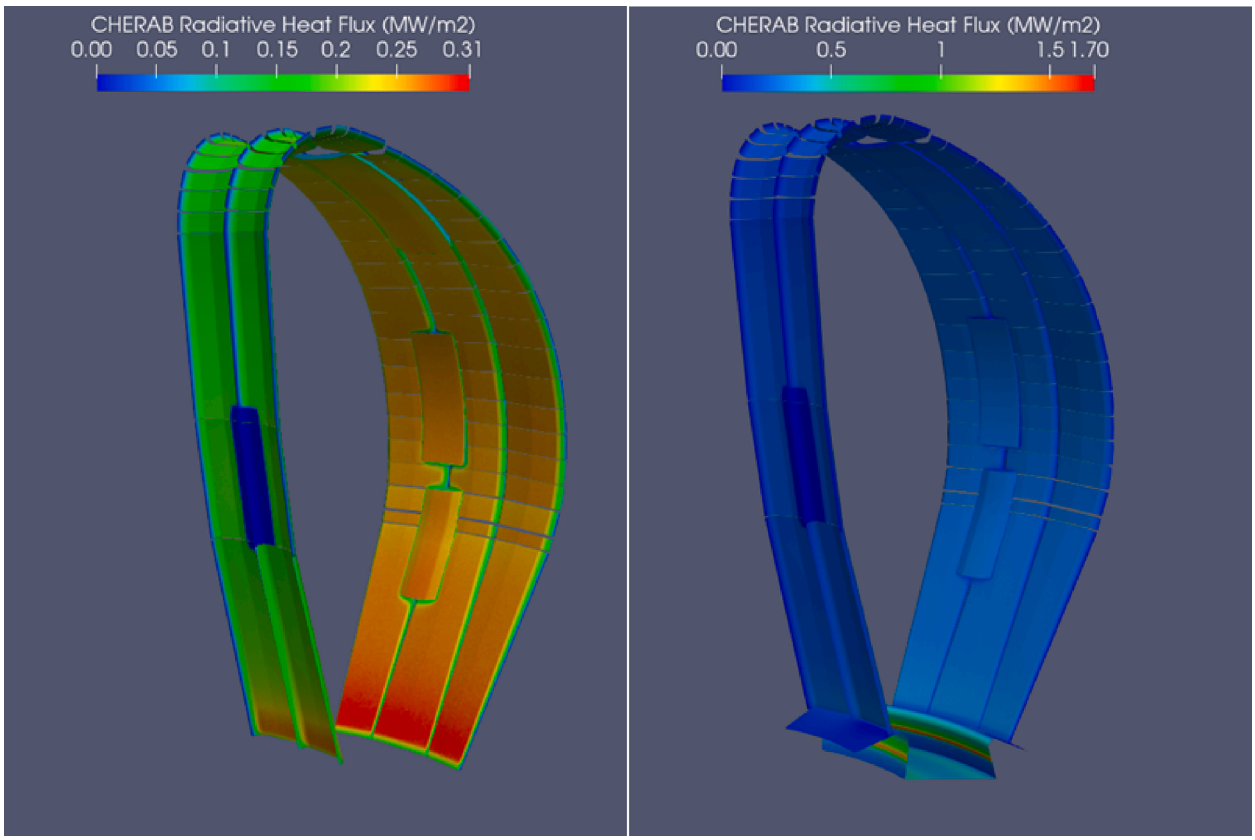

Fig. 5. Heating power distribution on the FW of a EU-DEMO sector when considering both core and SOL source . The figure on the left does not depict the divertor region in order to allow a focus on the FW blanket modules (note also the different colour scale among the two figures).

behind it). Clearly, this peak radiation load is mainly due to the radiation front in the SOL to ensure detachment, which is located close to the target plates.

- When the FW only is considered, the heat load is observed to remain everywhere below the technological limit of 1 MW/m^2 with sufficient margin. In the opinion of the EU-DEMO team, this margin is sufficient to absorb the impact of both the uncertainties in the radiation source as well as eventual poloidal and toroidal peaking factors, which have not been considered here.

It can therefore be concluded that the electromagnetic radiation from the plasma does not represent a major risk for the PFC integrity during the steady-state phase in the current EU-DEMO design, and thus it does not require dedicated design solutions.

3.1.2. *Charged particles*

Radiation does not represent the only source of heat load on EU-DEMO. In fact, thermal power also leaves the plasma in form of charged particles, which are absorbed on the surface of PFCs and therefore contribute to the total heat flux. In absolute terms, the power carried by charged particles is lower than the radiative one. Still, depending on the chosen magnetic equilibrium, charged particles may create hot spots where the local heat power overcomes the technological limit. Most of the charged particle power heads onto the divertor, also in view of the very narrow heat channel width (normally indicated with λ_q) expected for EU-DEMO according to the widely employed Eich scaling [32,33].

In order to be conservative though, the existence of a far-SOL heat channel, with a much broader $\lambda_q = 50$ mm has been assumed. This far-SOL channel (see Fig. 6) carries a power of 69 MW, corresponding to ~ 30% of the power crossing the separatrix – which in turn is assumed to be higher than the reference value to ensure robustness [22]. As mentioned, this is a quite conservative approach in order to absorb uncertainties, since the turbulent transport in the SOL, responsible for this second and broader channel, is believed to affect mostly the particle transport rather than the energy, as discussed for example in [34]. This approach is qualitatively in line with the ITER heat load specification (although a different far-SOL channel width has been assumed [35,36]).

To protect the FW from charged particle heat load both during steady-state and during transients (see next sections), the adopted design solution in EU-DEMO consists of installing poloidally and toroidally discontinuous, protruding limiters. These limiters, depicted in Fig. 7, are able to withstand a higher heat flux than the breeding zone since are not supposed to allow breeding behind them this obviously impacting on the overall breeding ratio. Details on the limiters design can be found in [6–8,37–39].

Function of the single limiters is discussed in the following sections, since those protruding structures are particularly important during transients.

The calculation of the peak heat load is carried out with the code PFCflux [40], a field-line tracing code able to map on the FW all the field lines at the OMP. Conservatively, the perpendicular transport of particles across the field lines, as well as the energy losses particles may undergo in their travel towards the wall, are neglected. The surface recombination energy deposition has been neglected as well.

Table 2 reports the maximum value of heat load both on each limiter and on the unprotected wall in start of flattop (SOF) and end of flattop (EOF) – the magnetic equilibria having been calculated with the code CREATE-NL [41,42]. Unsurprisingly, limiters exhibit a larger peak load, since they are protruding from the first wall and thus intersecting "earlier" the magnetic field lines.

More interestingly, the unprotected wall receives in the worst case about 0.5 MW/m^2 – this value being reached close to the divertor baffle. As discussed in the next sections, this is the region of the FW where,

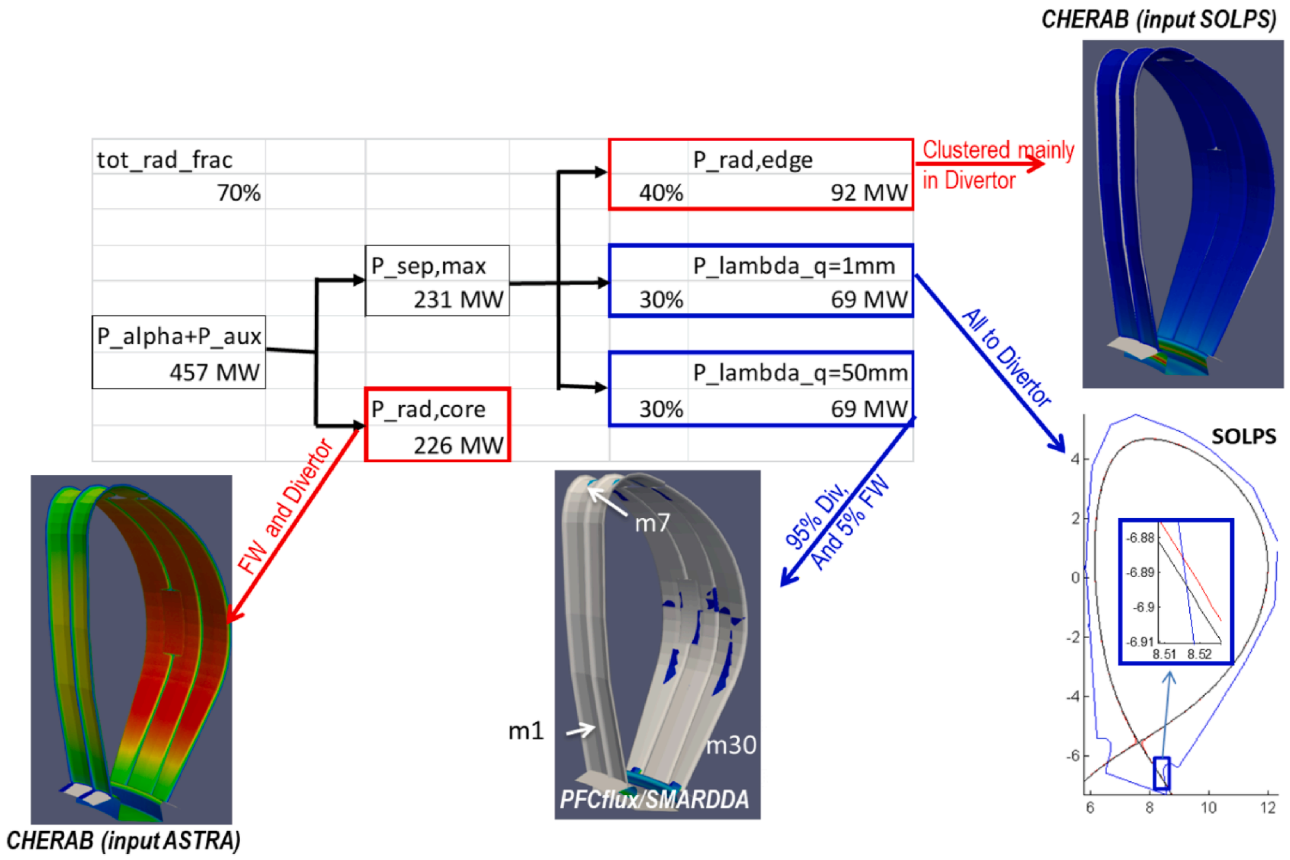

Fig. 6. Assumed subdivision of the heating power originating from the EU-DEMO plasma in the various channels (also, codes used for the various investigations are reported). This subdivision is extremely conservative (see main text), and has been adopted solely to evaluate the heat load on the FW due to charged particle transport. Note also that the power crossing the separatrix is larger than in Table 1, since the analysis concentrated on a conservative case. This figure is an adaptation of Fig. 1 in [22].

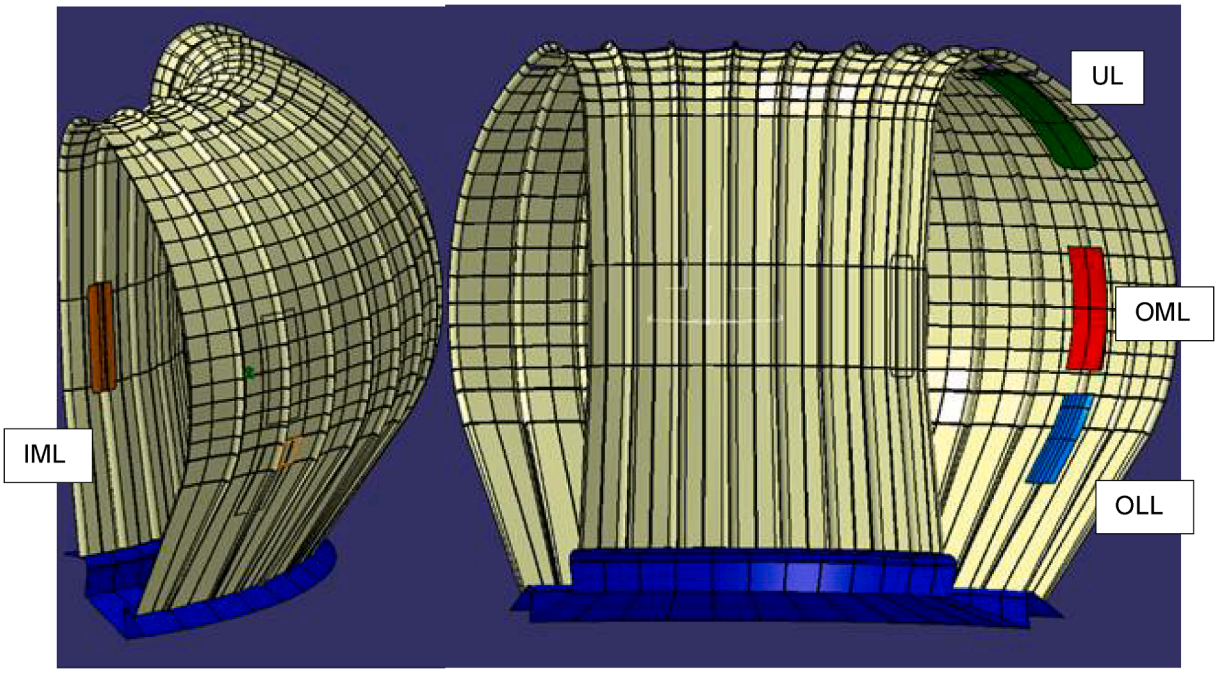

Fig. 7. Position of limiters in the current EU-DEMO design configuration. Brown: Inner Midplane Limiter (IML), Green: Upper Limiter (UL). Red: Outer Midplane Limiter (OML). Cyan: Outboard Lower Limiter (OLL). Colors may be visible online only. (For interpretation of the references to colour in this figure legend, the reader is referred to the web version of this article.)

Table 2
Peak heat load on limiters and FW due to charged particles. Since there are slight modifications in the magnetic equilibrium, both the start of flattop (SOF) phase, as well as the end of flattop (EOF) phase values are reported. Values of the heat flux are expressed in MW/m^2.

Scenario	Case	PSOL (MW)	λq (mm)	Deposition time	OML	UL	OLL	IML	FW
SOF	Diverted	69	50	Steady state	0.53	0.82	0.09	0	0.40
EOF	Diverted	69	50	Steady state	0.54	1.01	0.1	1.84	0.48

typically, the highest heat loads concentrate. It may be possible then, that a sort of "reinforcement" could be necessary there. Overall, as shown in Fig. 8, the FW is to a very large extent protected by charged particles by the screening of protruding limiters.

Fig. 9 shows the sum of radiative and charged particle loads. Thus, even in this very conservative case where the far-SOL power channel has been largely overestimated, the sum of the radiative heat load and the charged particle heat load remains everywhere below the technological limit of 1 MW/m^2, this providing good indications on the robustness of the concept. It is anyway important to stress that the charged particle deposition, contrary to the radiative heat flux, is extremely sensitive to both the magnetic equilibrium and the wall shape. Optimisation activities have been carried out on the present machine design, but an eventual change in the machine configuration needs therefore a repetition of the analyses presented here – although the values found allow for some optimism.

The analysis reported in this section does not account for fast particles losses, both from NB injection and fusion α's. Actually, all investigations carried out inside the EU-DEMO team on this topic have shown that losses and, correspondingly, associated loads on the PFCs are in reality quite small. This is due both to the low field ripple the machine is designed to have, and, foremost, to the quite large clearance between the plasma and the wall (about 22.5 cm on the OMP [22]). For α's, in addition, the large size of the machine plays a role in reducing the prompt losses. Published studies [43] have found the heat load on the FW associated to NB losses to be largely below the technological limits (i.e. ~ 40 kW/m^2). More recent, unpublished studies have shown that this applies even in presence of a plasma separatrix corrugation due to MHD activity – i.e. the EHO characterising QH-mode discharges [44]. Also, it has been shown that α's losses remain negligible even in the simultaneous presence of a large sawtooth crash and NTMs [45]. Finally, the interplay with TAEs, BAEs and other MHD modes triggered by fast particles is not believed to be an issue with this respect, since these modes may affect the efficiency of the core plasma heating by redistributing α's, but not the associated loads on PFCs, again by virtue of the large size of the device. No conclusive studies are available on this latter point though, because of the high sensitivity of these modes on the core kinetic profiles, which at the moment are not robustly established.

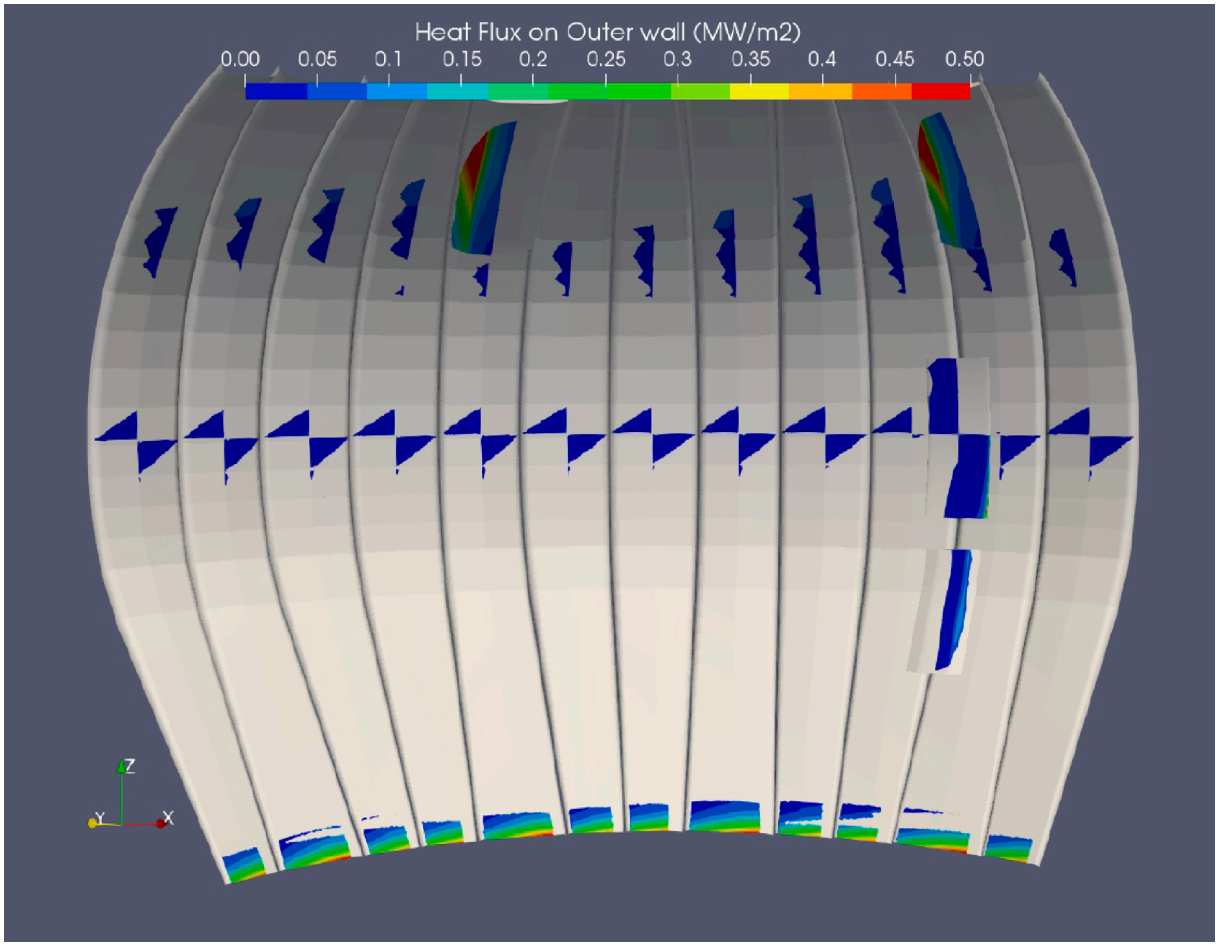

Fig. 8. Distribution of charged particles heat load on the outer DEMO wall. A very large fraction of the unprotected first-wall is effectively screened by the limiters, which take the largest amount of particles. The highest flux on the bare wall is found close to the divertor baffle.

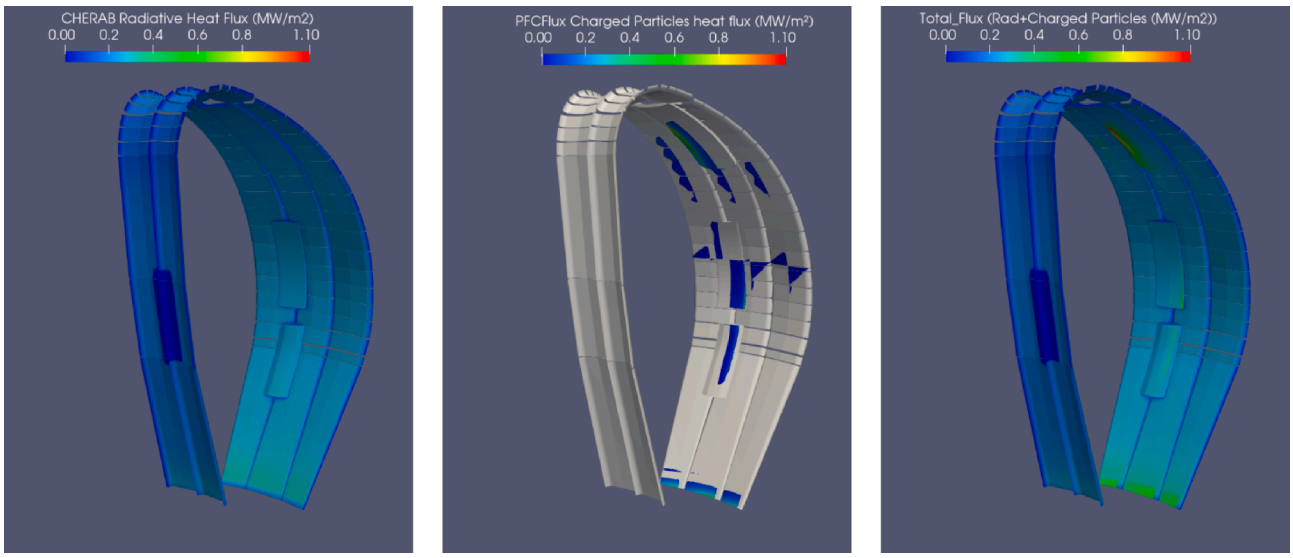

Fig. 9. Radiative heat flux (left), charged particles heat flux (SOF - mid) and resulting total heat flux (right) in a EU-DEMO sector.

3.1.3. *Neutrals*

The third source of heat flux during normal operation steady-state is represented by neutral particles. Of particular worry are the high energy neutrals originated by charge exchange (CX) reactions in the DEMO pedestal region, which can reach an energy of the order of keV and be thus quite effective in terms of wall erosion. It has in fact been shown e. g. in [46] that most CX events take place in the pedestal region, and those neutrals are the most dangerous in terms of sputtering yield. Fig. 10 – which corresponds to Fig. 4 in the quoted reference shows that the higher the pedestal temperature, the higher the corresponding sputtering yield of the CX neutrals. A preliminary evaluation of the impact of these high energy neutrals can also be found in [47,48], but more detailed investigations are at the moment ongoing.

For this issue, no real design countermeasures are at this stage foreseen. Possibly, a limit on the allowable pedestal pressure (i.e. a reduction in temperature, while trying to keep the density sufficiently high) in the plasma scenario definition might be at some stage introduced, this potentially having an impact on the achievable fusion power.

3.2. *First wall protection – transients*

One of the main lessons learned in the pre-conceptual design phase of EU-DEMO is that the transients have a much stronger impact on the machine design than the quiescent flat-top phase. There are broadly speaking two different categories of transients:

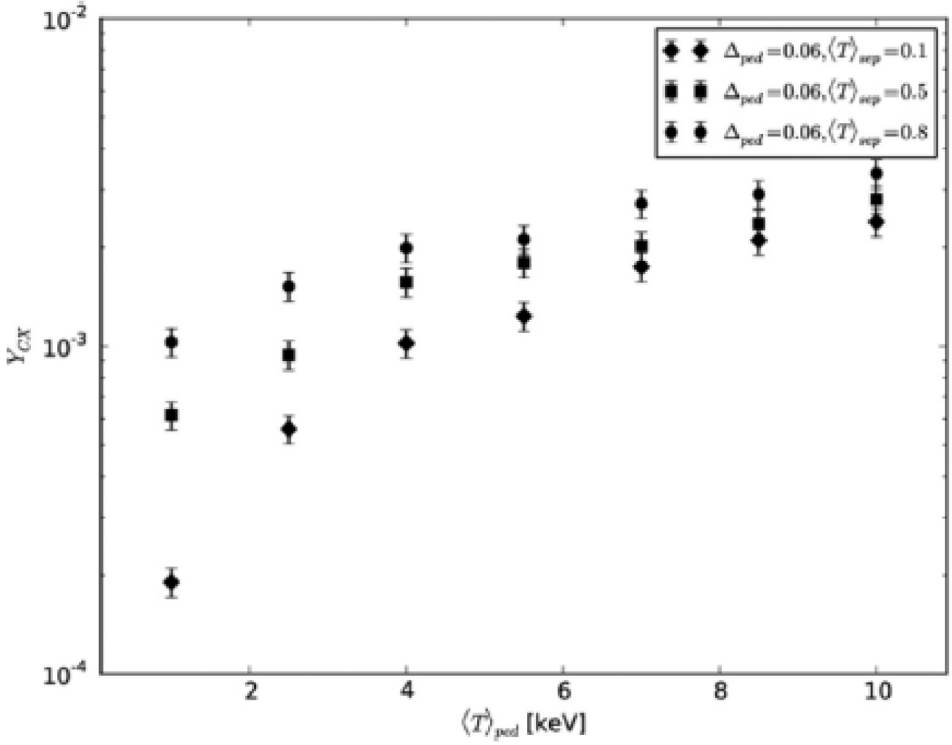

Fig. 10. Sputter yield of wall impinging CX neutrals vs. pedestal top temperature for separatrix temperatures of 10 0/50 0/800 eV. Figure is taken from [46].

- *Planned transients*: with this expression are here indicated the current ramps to access the flat-top phase and to exit it. It is herewith recalled that EU-DEMO is a pulsed machine [2]. Thus, the ramp trajectories have to possess a high robustness, since they will be repeated numerous times (tens of thousands) in the course of EU-DEMO operation.
- *Unplanned transients*: with this expression are indicated all transients which, ideally, are never taking place during EU-DEMO operation, but which nevertheless can occur, and mitigation actions have to be foreseen in order to protect the investment. These include, for example, mitigated and unmitigated disruptions, H-L transition past an uncontrolled (but slow) loss of confinement, divertor reattachment and ELMs, which deserve however a separate treatment.

During plasma ramps, a contact (at low current) between the plasma column and the limiters is foreseen. Also, a plasma/wall contact is unavoidable in case of disruption (although the plasma control system is required to avoid this occurrence by slow losses of confinement and in case of divertor reattachment – an overview on DEMO plasma control concept can be found in [49,50]). The situation is summarised in Fig. 11, a thorough discussion of the various phases is instead provided in the following subsections.

3.2.1. Planned transients

In EU-DEMO, plasma breakdown takes place close to the inboard (with EC assistance), then the plasma column moves towards the outboard and touches OML (see Fig. 11) before entering the diverted configuration [6]. According to the current ramp trajectories analysed, the plasma remains in the limiter configuration up to ~5 MA of plasma current. Fig. 12 shows the magnetic equilibrium for $I_p = 3.5$ MA.

Again following the ITER heat load specification, it is for simplicity assumed that, during the first phases of the ramp,

$$P_{heat}[\mathrm{MW}] \approx I_p[\mathrm{MA}] \tag{1}$$

which implies that the full auxiliary, non-ohmic heating of the plasma starts only after the achievement of the diverted configuration, in order not to exacerbate the PFC protection issue. Also, the heat channel width λ_q is supposed to be much larger than the steady-state value, in view of the reduced plasma current. These assumptions are based on the results of COMPASS and JET [51,52,53], as explained in [22].

The charged particle load on the OML during this phase is shown in Fig. 13. The peak value – which is located at the side of the OML, where the edge is sharper – is found to be around ~ 1 MW/m^2, i.e. an order of magnitude below the technological limit, which for OML is analogous to the divertor target, being the only actively cooled limiter (other limiters are "energy dampers" for disruptions, and are never involved during planned transients). Note that this case is the worst case produced in a sensitivity scan for different heat channel widths, in order to evaluate the effect of uncertainties on that quantity. This calculation clearly shows the necessity of such a limiter, since this situation on the bare wall would be too close to the maximum allowable flux to be considered acceptable.

During ramp-down, the most solicited part is the inner limiter, especially in case a strong turbulent transport in the SOL still exists (magnetic equilibria not shown here for the sake of brevity). Currently, the ramps trajectories for EU-DEMO are still subject of optimisation, and the shape and current evolution is now investigated together with transport effects (e.g. with ASTRA or RAPTOR [54]). However, the large margin on the heat load gives confidence on the suitability of the present concept.

Table 3. Summarises the peak values on the limiters and on the first wall for ramp-up and ramp down. As one can see, the outer limiter protects the wall during ramp-up, while the inner limiter is mostly loaded during ramp-down in the (unlikely) case strong SOL turbulence is present. An important point which requires dedicated analyses is however the W erosion during the plasma-limiter contact in the ramp-up. In the limiter phase in fact, the eroded tungsten would immediately enter the confined plasma region, having potentially catastrophic consequences on the stability of the ramp, and also on the necessary H&CD power to access flat-top. This point is currently under investigation.

3.2.2. Unplanned transients

The unplanned transients in general represent the highest risk for the machine integrity in EU-DEMO, in view of the large amount of kinetic and magnetic energy that the EU-DEMO plasma contains (about ~ 3 GJ, approximatively equally distributed between kinetic and magnetic). The

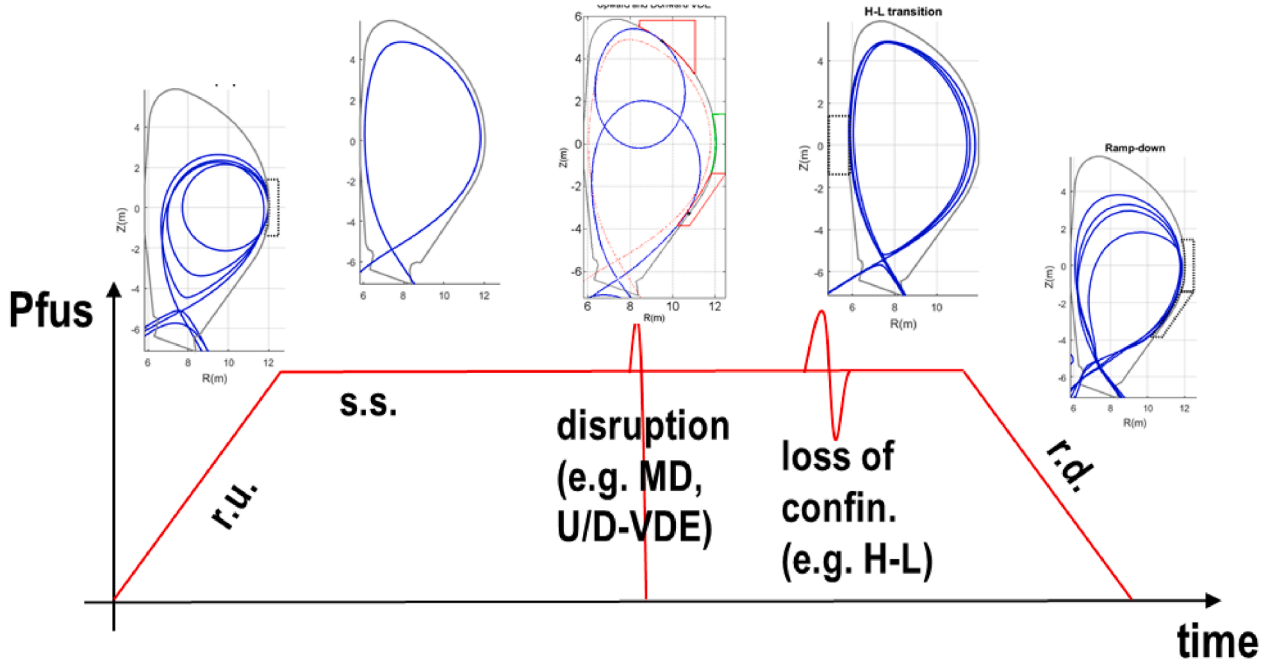

Fig. 11. Role of the various limiters in the different phases of the EU-DEMO plasma discharges, Here, also unplanned transients (disruptions and unwanted H-L transition) are depicted, although they are clearly not expected to take place in every discharge.

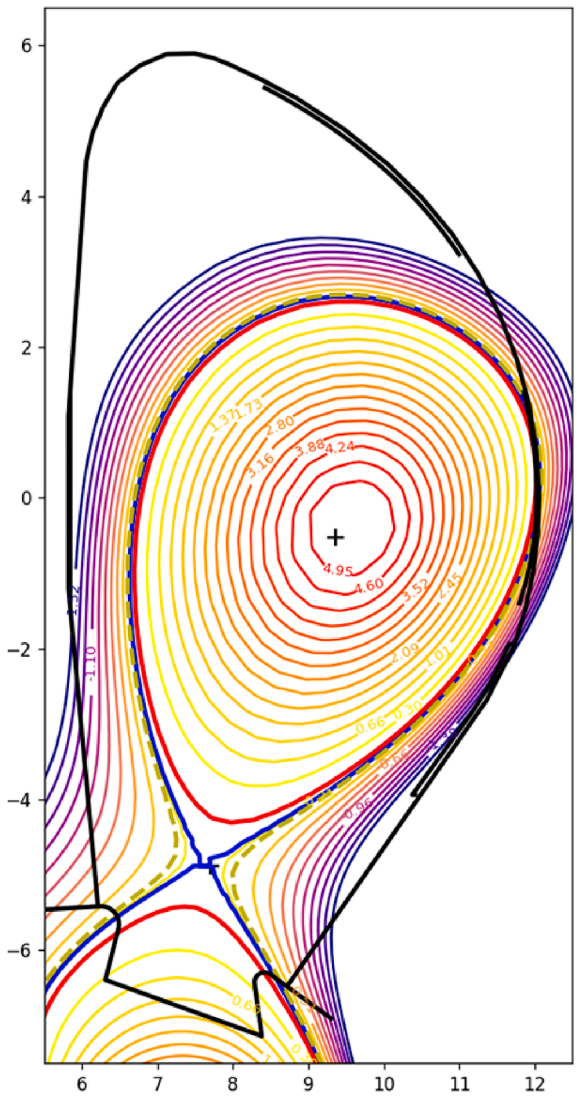

Fig. 12. Magnetic equilibrium for EU-DEMO during ramp-up at$I_p = 3.5$ MA, i.e. during the transition between limiter phase and diverted phase.

main effort in the DEMO design is to identify a plasma scenario which is as less prone as possible to these kind of events, or, complementary to that, design a control system and an actuators set-up able to avoid a disruptive evolution of the plasma discharge in the largest number of cases. Nevertheless, the machine has to be designed to passively minimise the consequences of a disruption, in case avoidance fails. This is possibly the main role of limiters. The underlying idea is that every disruptive event, no matter the dynamics, will end up by depositing the (very large) charged particles heat load on one limiter (or, better, on a high heat flux component), leaving the bare breeding wall untouched, or anyway taking fluxes below the critical values possibly leading to in-vessel LOCAs, where LOCA is the acronym for Loss Of Coolant Accident, and indicates a leak of coolant, in this particular case into the plasma chamber. In particular:

- Central disruptions will deposit the heat load on the divertor.
- Upwards VDEs will deposit the heat load on the upper limiter UL.
- Downwards VDEs will deposit the heat load on the outer lower limiter OLL.
- Losses of confinement (which can cause the plasma torus to sink as a consequence of the Grad-Shafranov equation) would lead, if uncontrolled, to a plasma-wall contact on the inner midplane limiter IML.

Consequences of an in-vessel LOCA are expected to be quite catastrophic. A preliminary evaluation can be found in the EU-DEMO IDM under [55]. In fact, in case of LOCA, the affected component shall be replaced, various tests have to be carried out and VV shall be conditioned again. An interruption of operation of several months has to be accounted for in case of LOCA, which may be even longer in case multiple blanket modules are affected (for an overview on the EU-DEMO blanket maintenance concept, the reader is referred to [56]). Note that, in view of the extremely large heat loads which are developed during a disruption, the limiters are not supposed to not be damaged. Their "sacrifice" protects however the rest of the machine, avoiding e.g. in-vessel LOCAs or damages which will force a very long operation interruption. In fact, these limiters are supposed to be relatively easily accessible for remote maintenance, thus making their replacement more manageable than repairing a damaged breeding module [6,57–59]. Preliminary assessments (unpublished) indicate few weeks for limiter replacements (depending also on the position), compared to 3–6 months a damaged BB module replacement may require. Note also that, in case of several BB segments being damaged, it is unlikely that many replacement segments would be available in stock. Plus, these components are designed in such a way that even a catastrophic event would not damage the coolant channels, as it would on the unprotected wall in view of the reduced wall thickness. Finally, it has to be noted that limiters may even still allow the continuation of the operation without opening of the vessel, if the damage is limited. This needs however the development of an inspection technique not requiring the opening of the vacuum vessel itself, in order to verify the acceptable condition of the limiters. This has of course a very positive impact on the overall machine availability.

For brevity, it is here impossible to show all cases which have been analysed. All peak values on the wall and on the limiters can be found on Table 4. Also, the magnetic equilibrium evolution during an upper VDE, as well as the corresponding heat flux values on the first wall, are shown in Figs. 14 and 15 respectively. The effectiveness of the limiters to protect the heat load from excessive overheating emerges clearly.

It is easy to show that when considering the heat load factor (i.e. energy surface density divided by the square root of the discharge duration), in all cases the value of 50 $MJ/m^2/s^{1/2}$ – corresponding to the presence of melted tungsten – is largely exceeded on the limiters.. Also, for the upper VDE, there is again a large heat flux on the FW close to the baffle region, which, as discussed before, needs to be reinforced as well.

A very important open question is to understand whether limiters are indeed able to protect the wall from all possible transients, or if there are still events where the plasma can move in unpredictable directions and land in unprotected regions of the machine (e.g. in presence of strong toroidal and poloidal asymmetries in the plasma column). This point is currently under consideration in the DEMO team, with the involvement and support from various specialists. Also, this may require to change the foreseen number of limiters to be introduced - at the moment, limiters are foreseen at 4 different toroidal locations, i.e. 16 installed limiters in total. It is important to stress that an high number of limiter, although beneficial for the wall, might compromise the T breeding capability of the machine.

Concerning active disruption mitigation, there is at the moment no concept foreseen for EU-DEMO which differs from what prescribed for ITER. This might change in the next EU-DEMO design phases, especially if new results are produced by the scientific community.

It is here however incidentally noted that a too "effective" mitigation of the disruption, namely a complete conversion of the plasma energy into radiative power homogeneously distributed onto the entire first wall, might also not be suitable for DEMO, since the radiation load might anyway be too high to exclude damage to the unprotected wall (the so-called *radiation flash*). This aspect is also under consideration in the ongoing EU-DEMO design activities.

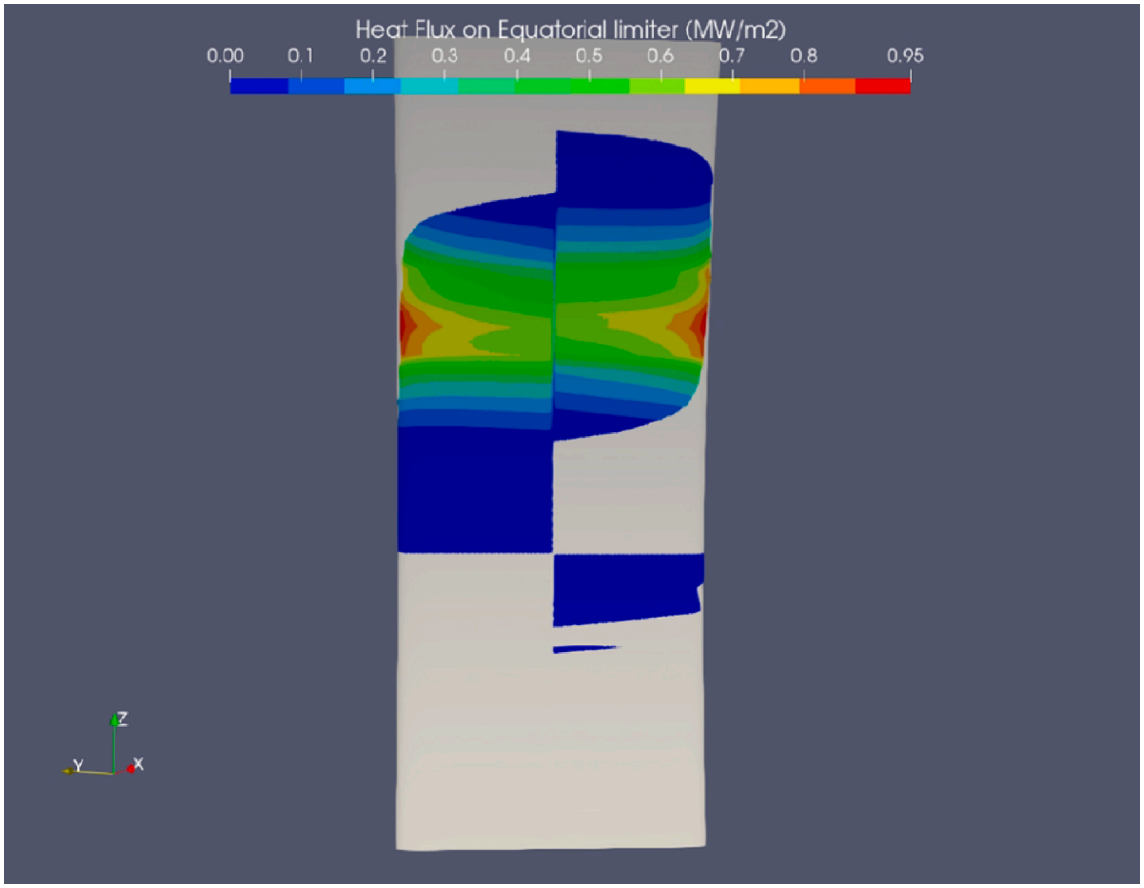

Fig. 13. Charged particles heat flux on the OML during ramp-up atI_p = 3.5 MA, i.e. during the transition between limiter phase and diverted phase.

Table 3
Peak heat load on limiters and FW due to charged particles during ramp-up and ramp-down for different values of the current and different assumptions on λ_q. The data in the last five columns are expressed in MW/m^2.

Scenario	Case	PSOL (MW)	λq (mm)	Deposition time	OML	UL	OLL	IML	FW
Ramp-Up	Limited	3.5	6	17.5–35 s	2.37	0	0	0	0.29
Ramp-Down	Limited	5	6	25–50 s	<0.01	<0.01	<0.01	0.02	0.01
		5	50	25–50 s	<0.01	<0.01	<0.01	1.39	0.60

3.2.3. *Runaway electrons*

Runaway electrons (REs) are probably one of the main open issues in the EU-DEMO design. It is in fact at this stage very difficult to predict where the runaway beam is depositing its energy, since it may crucially depend on the MHD stability of the beam itself.

If the beam remains coherent, it is then safe to assume that all runaway electrons will deposit their energy on the limiter plates or on the divertor, which are by design intersecting the magnetic field lines before the rest of the first wall. Instead, if a kink instability distorts the runaway beam, symmetry might be broken, and sudden releases of high energy electrons onto the unprotected wall cannot be excluded.

Furthermore, the energy carried by REs could be too high to be tolerated by the limiters. In fact, if the REs penetrate down to the coolant channels and damage them, leading to an in-vessel LOCA, the concept would not accomplish its mission and the design must be changed (this doesn't happen during TQs, since the heat load is indeed very high but unable to penetrate as deeply in the component as relativistic electrons would, causing therefore mainly superficial damage).

No clear evaluation of the damage to be expected by REs is at the moment available. These studies will be carried out in the next phases, as well as the definition of a strategy to control the runaway beams in case its appearance cannot be by other means avoided, in order to ensure that even in presence of these dramatic events the integrity of the first wall is maintained.

Once more, it is here recalled that a primary goal for the EU-DEMO design is the identification of a plasma scenario where disruption are – ideally – absent.

4. Divertor compatibility

4.1. *Steady-state*

As stated in the introduction, the EU-DEMO Baseline configuration foresees an ITER-like lower single null divertor configuration. Possible alternative configurations, such like Snowflake, Super-X or double null, are currently under investigation, both with respect to the benefits in terms of power exhaust they may bring and concerning the compatibility with the engineering constraints (e.g. remote maintainability). Such alternative configurations have been subject of dedicated reviews in this conference. The reader is therefore re-directed there, as well as to past publications [9,10,60,61] for more details.

As already recognized from the very beginning of the dedicated

Table 4
Peak heat load on limiters and FW due to charged particles during different unplanned transients for different values of the current and different assumptions on λ_q. Values of the heat flux in the last five columns are expressed in MW/m^2, bold values (with yellow background) are expressed in GW/m^2. Values marked with * indicate an artificially down-shifted equilibrium with larger power at the separatrix, considered as a worst case.

Scenario	Case	PSOL (MW)	λq (mm)	Deposition time	OML	UL	OLL	IML	FW
U-VDE	First touch	69	1	20-35ms	<0.01	114.2	<0.01	0	0
		69	5	20-35ms	<0.01	15.6	<0.01	0	0.02
	TQ	**325**	7	1-4ms	<0.01	**63.6**	0	<0.01	138.2
	Current Quench	10	10	74-200ms	<0.01	2.52	0	<0.01	0.01
		10	30	74-200ms	<0.01	1.53	0	<0.01	0.11
D-VDE	First touch	10 (*69)	10 (*1)	15-35ms	<0.01 (*<0.01)	0 (*0)	<0.01 (*24.8)	<0.01 (*<0.01)	<0.01 (*<0.01)
		10 (*69)	30 (*5)	15-35ms	<0.01 (*<0.01)	0 (*0)	<0.01 (*7.83)	<0.01 (*<0.01)	0.08 (*0.01)
	TQ	**325**	7	1-4ms	0.77 (*182)	0 (*0)	**4.4** (***306**)	0.84 (*11.3)	8.11 (*292)
	Current quench	10	10	74-200ms	<0.01 (*<0.01)	<0.01 (*0)	<0.01 (*<0.01)	<0.01 (*<0.01)	<0.01 (*<0.01)
		10	30	74-200ms	<0.01 (*<0.01)	<0.01 (*0)	<0.01 (*0.07)	<0.01 (<0.01*)	<0.01 (*<0.01)
H-L transition	Limited (inboard)	30	2	1-5s	<0.01	<0.01	<0.01	338	0.23
		30	4	1-5s	<0.01	<0.01	<0.01	147	2.2
Major disr.	TQ	**325**	7	1-4ms	0.61	1.38	0.84	**8.57**	336
	CQ	10	10	74-200ms	<0.01	<0.01	<0.01	0.01	<0.01
		10	30	74-200ms	<0.01	<0.01	<0.01	0.21	0.05

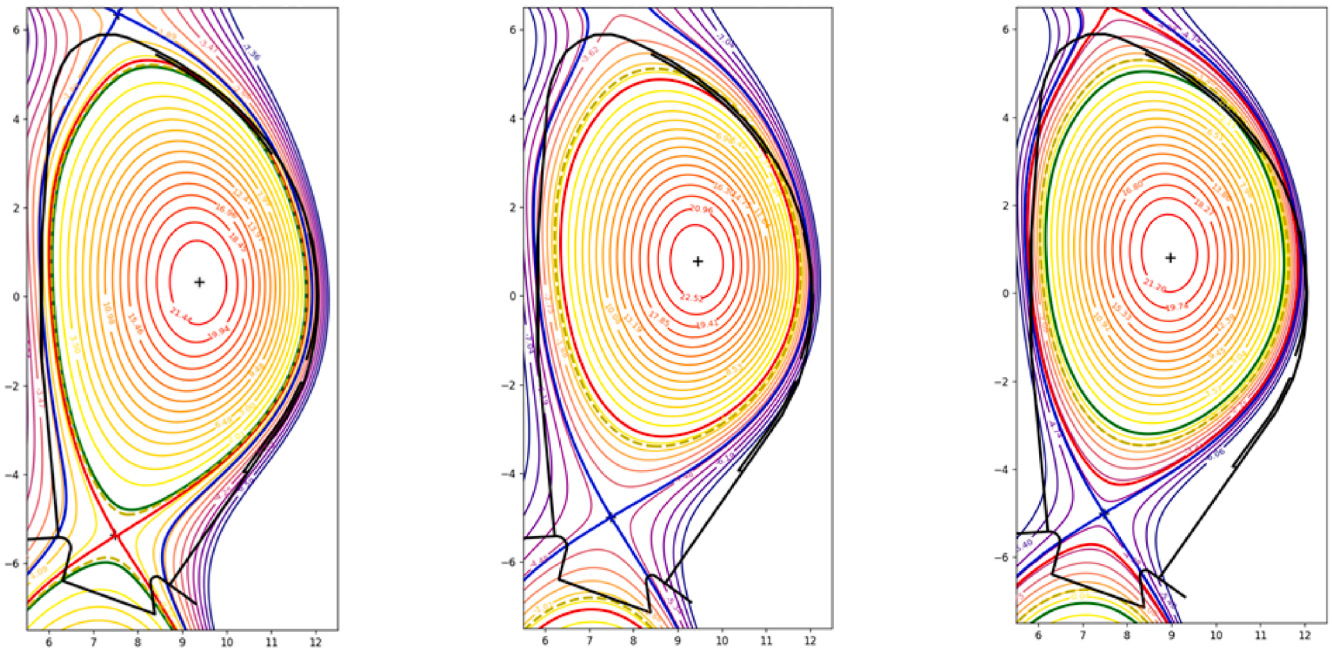

Fig. 14. Plasma magnetic configuration for EU-DEMO by an upper VDE – left: first touch (FT), centre: Thermal Quench (TQ), right: Current Quench (CQ).

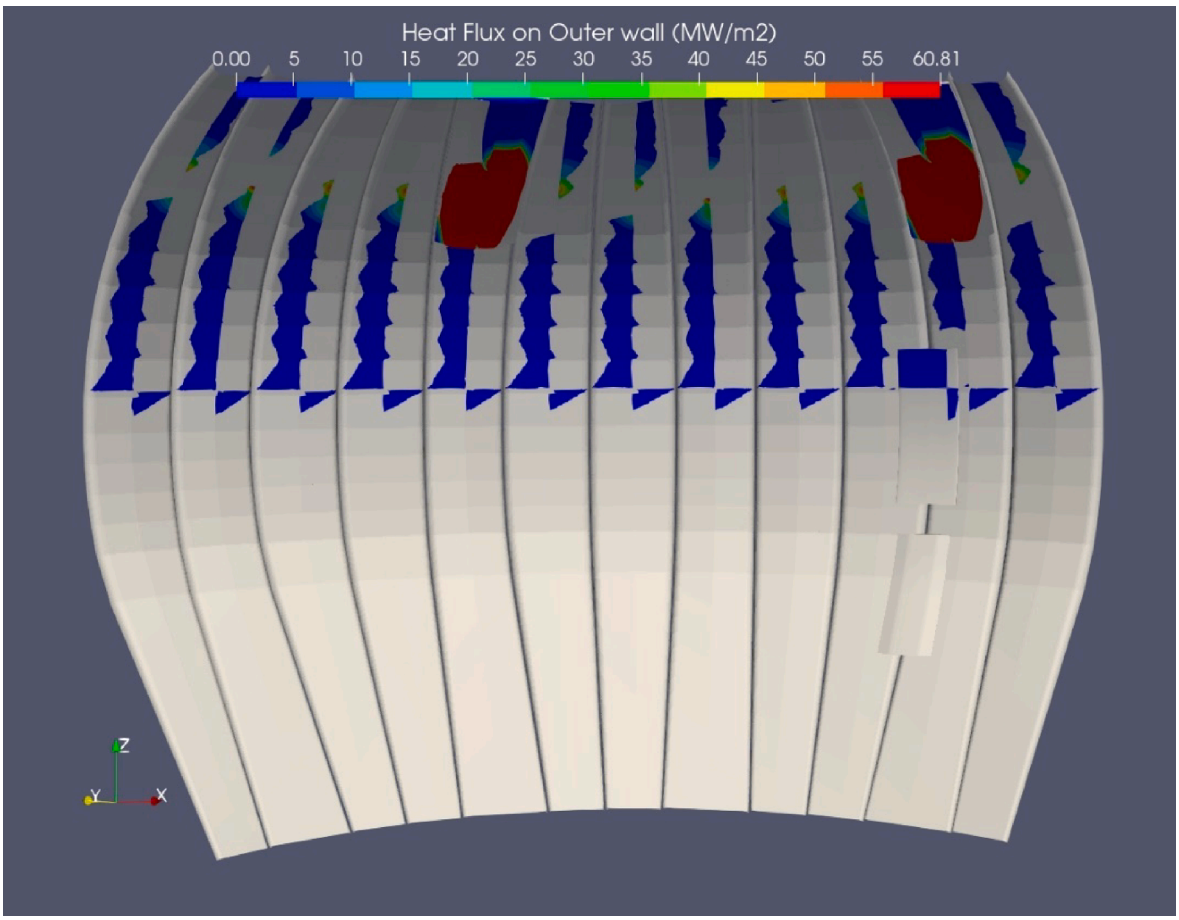

Fig. 15. Charged particles heat flux on the entire FW on a EU-DEMO sector during an upper-VDE event. The ability of limiters to protect FW is clearly visible.

investigations [22,62], the EU-DEMO divertor has to be operated in a detached state, as the heat flux in attached conditions is foreseen to be higher than the technological limit of 10 MW/m^2 by a factor up to 10 in the most severe cases. Fig. 16 shows a typical heat flux deposition profile calculated with SOLPS for a deeply detached case. As one can observe, in such situation the heat flux is everywhere safely below the engineering limit. With this respect, the EU-DEMO solution is qualitatively identical and quantitatively analogous to ITER [63].

A robust EU-DEMO integrated divertor solution shall satisfy simultaneously various requirements (here, "integrated" means that the fulfilment of these requirements do not depend solely on the divertor, but on the reactor design in a broader sense). These are for example:

- Allow for an efficient He removal, at a rate equal to the He generation from fusion power reactions in order to allow for a steady state operation. At the same time, this shall take place by maintaining the He concentration in the core lower than values where the fuel dilution starts to be significant (i.e. ~ 10%) [64].
- Allow for the existence of a detached solution with a density at the separatrix not larger than ~ 0.5 n_{GW}, or in general preventing the plasma confinement and/or its stability to deteriorate [65].
- Allow for the existence of a detached solution without recurring to an excessively high seeded impurity concentration, which can have negative repercussion on the main plasma (again in terms of energy confinement, fuel dilution or stability).

Large parameter scans with fluid neutrals performed with SOLPS have shown that working points fulfilling all these requirements possibly exist, but the operational margins are very narrow. Uncertainties associated to such calculations are however quite significant, also because there is at the moment nothing to benchmark them against – neither simulations with kinetic neutrals nor, obviously, experimental data. Nevertheless, there is a certain confidence in the fact that at least trends are correctly captured. For the next phases, more detailed modelling by means of SOLPS simulations with kinetic neutrals, which in turn will be used as input for other codes, are foreseen, in order to characterize in a greater detail such operational space and its controllability. It should be however pointed out that kinetic cases do not fully solve the problem related to the uncertainties on the plasma transport coefficients, which have a relevant impact on the results. First results of kinetic SOLPS for EU-DEMO are presented in this conference [28]. For these calculations, acceleration schemes as proposed in [66] have been employed, in order to at least partially accelerate the convergence – this point being particularly relevant for large mesh with high resolution.

Further features which can improve the robustness and the accuracy of the results, and which have not been applied yet, are the inclusion of the fluid drifts as well as the extension of the computational grid to the first wall [67]. For the former point, ITER-related results seem however to indicate that the impact is not too significant for large devices [68,69].

4.2. Unplanned transients

As discussed in the previous section, a solution for the steady-state exhaust problem and compatibility with the engineering constraints seems to exist, once a robust detachment sets on. Clearly, the situation looks different if and once detachment is lost. Calculations performed with the thermal–hydraulic code RACLETTE [70] have shown that, in presence of a heat flux of the order of the one expected in EU-DEMO by reattachment (i.e. ~ 50–100 MW/m^2), the currently assumed

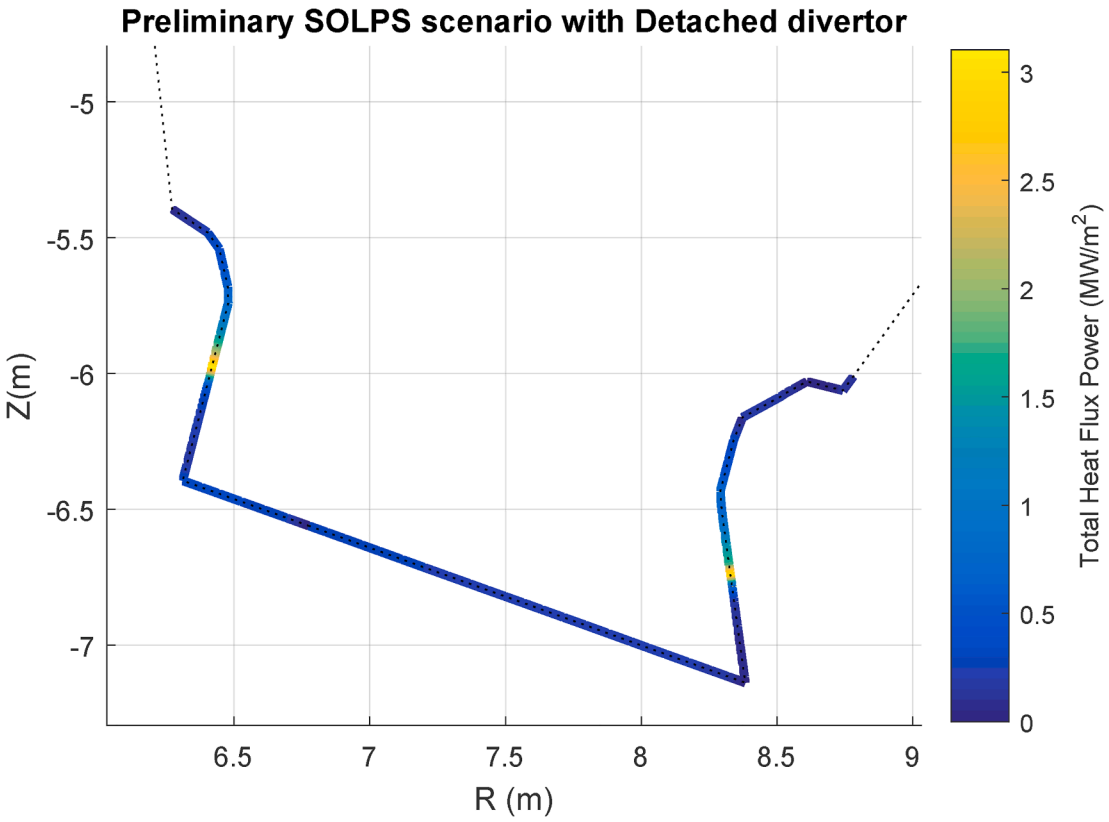

Fig. 16. Heat flux deposition profile calculated with SOLPS for the EU-DEMO divertor contour for a deeply detached divertor.

conventional single-null DEMO divertor can survive for several tens of seconds only in presence of divertor sweeping, reaching otherwise the burn-out condition in less than two seconds – see Fig. 17, the interested reader is referred to [11,71] for the details of the calculation.

In this case, the ITER solution of interrupting the plasma discharge by a fast shutdown (which corresponds *de facto* to a mitigated disruption) is not desirable, since EU-DEMO shall primarily be aiming at avoiding under all conditions a plasma-wall contact for the reasons elucidated above. For this reason, the possibility of sweeping the divertor as an emergency maneuver has been introduced in DEMO [11]. Sweeping would in fact allow to protect the divertor for a sufficient time to ramp the current down to an acceptable level for a fast termination to be performed, without recurring to an early, unacceptable plasma-wall contact.

The employment of the divertor sweeping has however a profound impact on the machine design. In fact, it necessitates:

- The presence of in-vessel coils (IVC). A possible, preliminary IVC configuration for divertor sweeping is visible in Fig. 18. In fact, the performance of a sufficiently fast (~1 Hz) divertor sweeping by the employment of ex-vessel coils turned out to be impossible. IVC however have a series of technological difficulties, not the least of which is their integration in the narrow space available. Also, the connected AC-losses limit the possibility of sweeping the divertor to about ~ 1 min [11], thus clearly indicating divertor sweeping being possible as emergency solution, and not for the unperturbed discharge.
- A diagnostic able to detect the occurrence of a loss of detachment before the heat flux at the divertor target reaches a dangerous value – also in view of the short time available to intervene. As discussed in [50], the selected solution is a spectroscopy concept able to follow the radiation front along the field lines in the divertor volume. This can (in principle) provide information on the detachment loss before it really occurs (e.g. when the radiation front is moving too rapidly towards the plates). Verification of the concept via synthetic diagnostic simulations is currently ongoing [14].

Also, the possibility of having a stable plasma ramp-down in presence of divertor sweeping is an open point, which requires further investigations.

4.3. Global impact of divertor on DEMO design space

In the past years, work has been dedicated to understand the impact of the divertor compatibility on the EU-DEMO design. In fact, the role of the divertor as a primary design driver has become apparent. Reinke [72] and Goldston [73] have shown that the concentration of seeded impurities to obtain detachment increases more strongly with the machine size than with the magnetic field. These results were confirmed by Siccinio et al. [74], who showed that reactor configurations with net electricity production and compatible with power exhaust only exist along a sort of hyperbolae in a $R - B_T$ plane, since at high field and size the excessive losses by synchrotron radiation degrade the energy confinement, whereas at low field and high radius the excessive seeded impurity to protect the divertor deteriorate the plasma confinement – as predicted by [72]. This is visible in Fig. 19 – taken from [74].

Fig. 19 was obtained by coupling ASTRA/Simulink with a simplified 0D divertor model [75], which was used to determine the necessary Ar concentration to reach detachment. Ar was supposed to migrate and contaminate the core as well, assuming a fixed ratio between the concentrations in the core and in the divertor (1:6). All points with non-zero electricity production represent converged solutions with detached divertor and $\boldsymbol{P_{sep}}$ comprised between $1.1P_{LH}$ and $1.2P_{LH}$ – i.e H-mode could be robustly sustained. In detail, Xe was added as core radiator when the power crossing the separatrix exceeded the upper limit, whereas auxiliary power was added in case the fusion power alone was not enough to maintain it above the lower limit. The net electric power P_{el} was estimated by

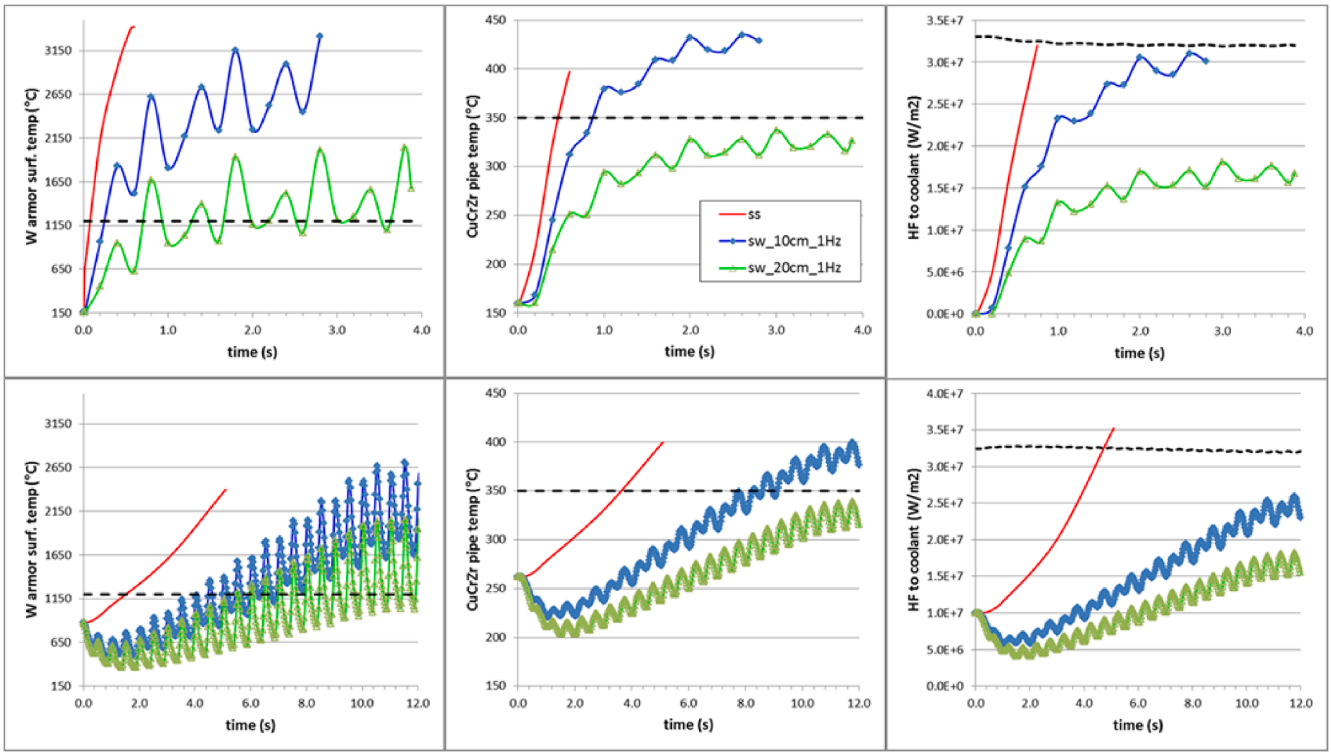

Fig. 17. RACLETTE simulation using as input 70 MW/m^2 heat flux. In the first row, a step variation in the heat flux from 0 to 70 MW/m^2 is assumed (with initial temperature T = 150 °C), whereas the second row refers to a 10 s ramp from 10 to 70 MW/m^2, this latter case assumed to be a more realistic approximation of a real loss of detachment. The curves refer to steady state (red), sweeping at 1 Hz of +/-5cm (i.e. 10 cm peak to peak – blue) and +/− 10 cm (i.e. 20 cm peak to peak - green), with considered limits represented as black dashed line. For both rows, from left to right, the following quantities are plotted: i) Temperature on tungsten armour (recrystallization limit = 1200 °C). ii) Temperature on CuCrZr pipe (softening limit = 350 °C). iii) Heat flux to coolant, with variable Critical Heat Flux limit. Note the different time durations of the calculations between first and second row. Figure is taken from [71]. (For interpretation of the references to colour in this figure legend, the reader is referred to the web version of this article.)

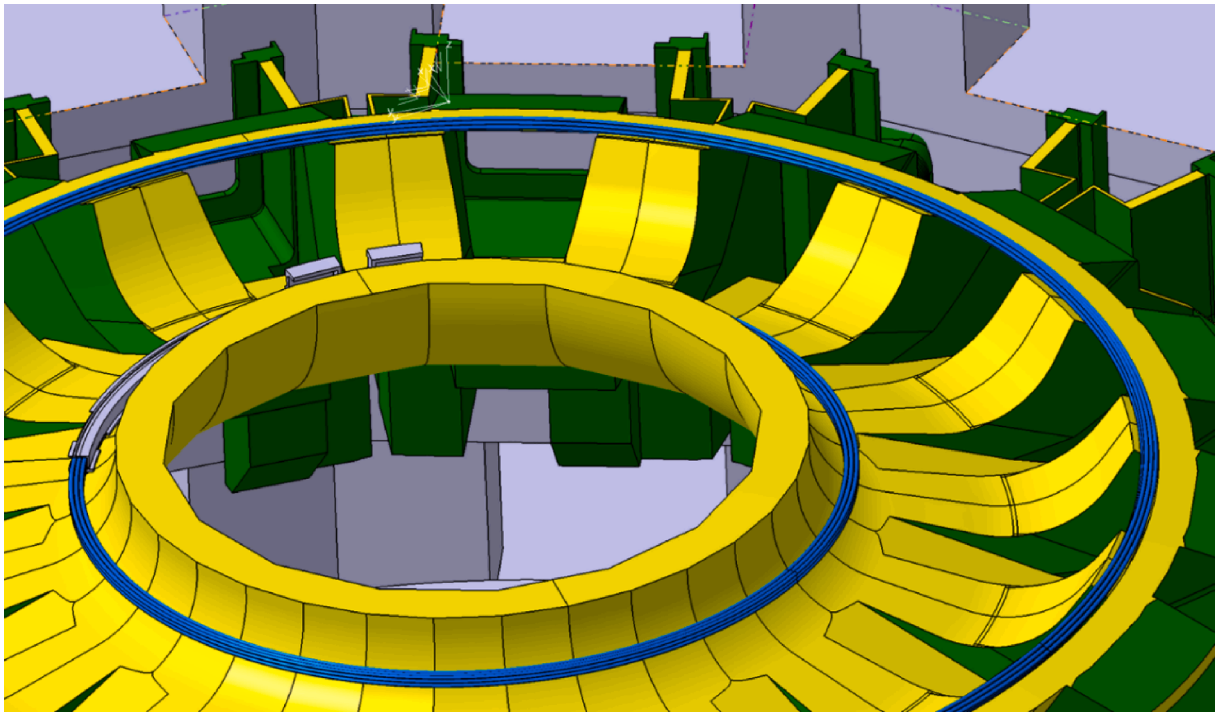

Fig. 18. Possible configuration of IVC for divertor sweeping after assembly. Coils are highlighted in blue. (For interpretation of the references to colour in this figure legend, the reader is referred to the web version of this article.)

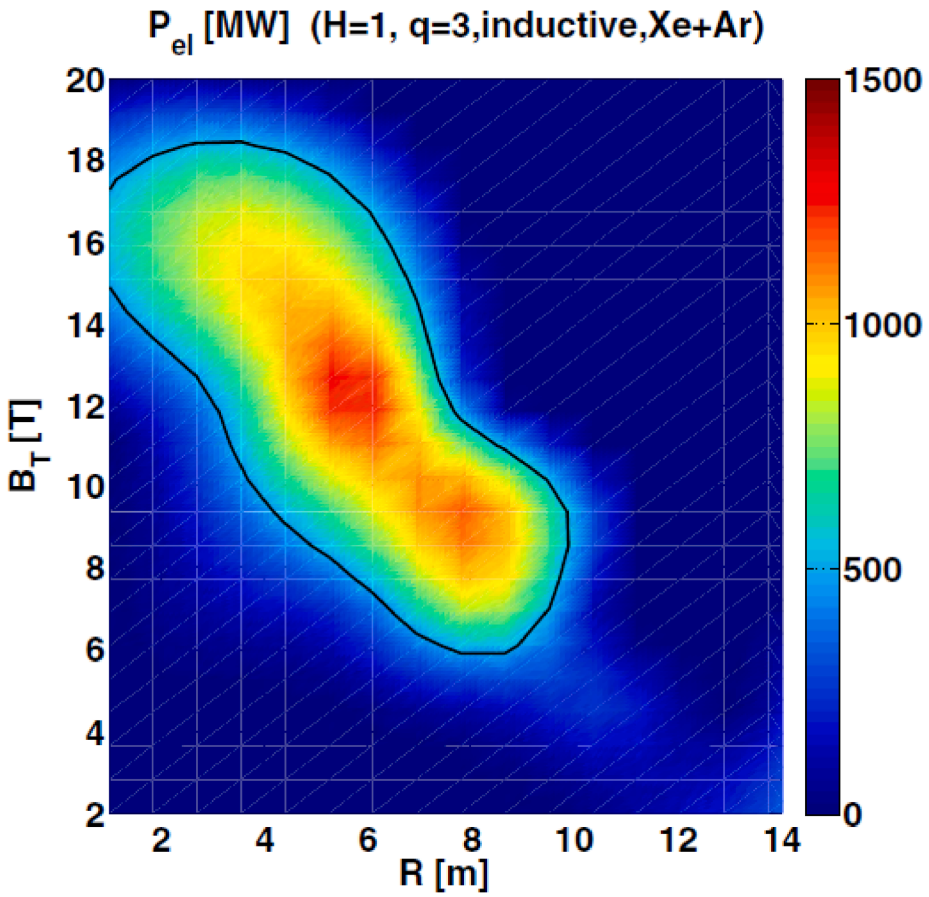

Fig. 19. Net electrical power for Xe + Ar cases (i.e. with divertor compatibility enforced) as a function of machine radius and on-axis toroidal magnetic field (at fixed safety factor and plasma shape). The black line highlights the *P*el = 500 MW level curve. Figure is taken from [74].

$$P_{el} = \eta_{th}\left(P_{fus} + P_{aux}\right) - P_{aux}/\eta_{WP} \tag{2}$$

where η_{th} and η_{WP} are the thermodynamic efficiency of the plant and the wall-plug efficiency of the auxiliaries, respectively, while P_{aux} is the necessary auxiliary heating power. Solutions at high radius and low field have a very low associated electricity production because of the very high Ar content which is necessary to protect the target, in (qualitative) agreement with the conclusions of Reinke. More recently, Siccinio et al. [71] pointed out that, when a technical constraint is added on the maximum allowable heat flux in presence of divertor reattachment, then the situation is more critical at higher field than at higher radius. In particular, it was pointed out that the heat flux at reattachment (or, more exactly, the thereto connected figure of merit $P_{sep}B/qAR$) scales like

$$\frac{P_{sep}B_T}{q_{95}AR} \propto f_{LH}{B_T}^{2.52}R^{0.16} \tag{3}$$

This means, in short, that the design space for DEMO – or for an FPP in general – is limited in terms of radius by the Reinke criterion, and in terms of field by ensuring divertor integrity in presence of reattachment events. Fig. 20 shows the available parameter space for reactor design when the limit originating from reattachment mitigation is superposed to Fig. 19 (assuming$f_{LH} = 1.2$ and assuming 70 MW/m^2 as technological limit, following Fig. 18). As one can observe, the impact of the latter effect is quite strong, since most attractive solutions in terms of electricity yield are now ruled out.

It is however important to stress that these results are only strictly applicable to an ITER-like LSN configuration with seeded impurity for power dissipation. Also, some of the physics assumptions employed - e.g. the factor 1:6 for the Ar compression factor, or the Eich scaling for the heat flux channel width - may turn out to be too conservative, this allowing for a relaxation of the constraints. Other divertor configurations may help in opening up the available parameter space, and ease the problem of finding an operative points both for DEMO and, especially, for the future FPPs (e.g. by ensuring that reattachment can under no circumstances take place).

5. ELMs

A simple estimate from a scaling recently suggested in Ref [76] indicates that, in EU-DEMO, a natural type I Edge Localised Mode (ELM) releasing 10% of the pedestal energy would deposit the equivalent of ≈ 10 MJ/m^2 of energy in around one millisecond on the target plate, corresponding to an heat load factor of about ∼ 300 MJ/m^2/s$^{1/2}$, i.e. significantly above the melting threshold. Simulations performed with the code RACLETTE [70] have in fact shown that even a single ELM event of this kind will be sufficient to cause surface melting of the W-coated target plate, and a few tens of these events will ablate half of the total thickness of the W layer. These results are consistent with the analysis in [77]. Also, it is not at this stage clear to which extent ELM shall be mitigated in a machine of the size of DEMO, where, possibly, a full suppression is needed, also in view of the duration of the discharges and the high frequency of the ELMs [63].

This risk poses a serious question mark on the suitability of ELMy H-mode as a reactor scenario, since a reliability of 100% would be required for any chosen ELM mitigation or suppression method, a challenging engineering target to meet (even disregarding other drawbacks all active ELM mitigation or suppression techniques might have on the plasma performance). For this reason, a plasma scenario which is naturally ELM-free, as for example the QH-mode [78], the I-mode [79], or even

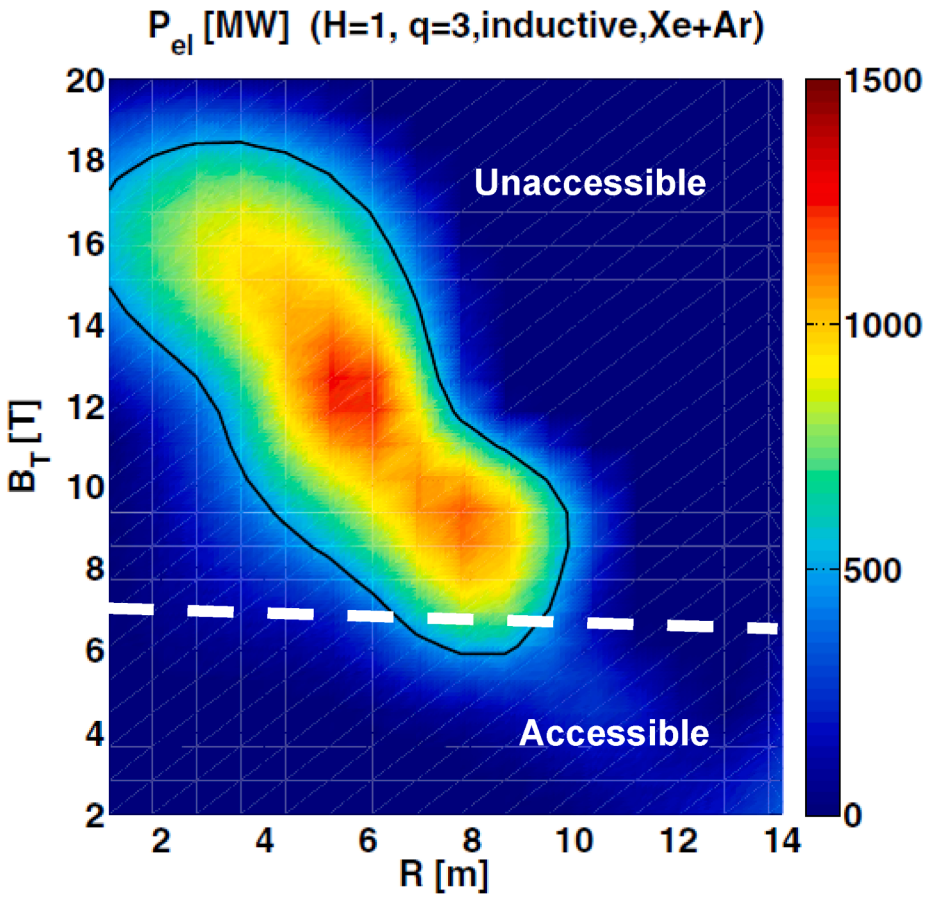

Fig. 20. Same as Fig. 19, with in addition the limit linked to divertor reattachment for a LSN configuration (white dashed line), assuming $f_{LH} = 1.2$. As shown in [71], such limit depends only weakly on the radius but strongly on the field strength.

negative triangularity [80,81,82] would be extremely beneficial for a machine like EU-DEMO, whose mission includes stringent availability requirements. More recently, other no- or small ELMs scenarios have been found [83,84]. It is here incidentally noted that an high-confinement plasma where ELMy activity is naturally absent would be of great advantage for the success of ITER as well.

The impact on the plant architecture following the adoption of one of these regimes may be extremely significant – with negative triangularity being possibly the most extreme example.

Due to the very preliminary status of the definition of a suitable, ELM-free plasma scenario in EU-DEMO, the discussion is here left on a generic level. The main message is that the need for strongly mitigating – or completely suppressing – ELMs may turn out to have the most impact on the EU-DEMO design, with consequences still uncertain at this level.

6. Conclusions

In this work, the impact of PFC protection needs in driving the EU-DEMO design has been reviewed, by describing the current status of the related EU-DEMO investigations and the motivations behind them – with the obvious caveat that the EU-DEMO design may still undergo significant modifications in the future.

Concerning the FW, the EU-DEMO solution is characterised by the presence of protruding limiters, which play the role of absorbing the largest fraction of heat carried by charged particles, both during steady-state and during planned and unplanned transients, thus protecting the thin breeding wall, especially during disruptions. These limiters have in fact been designed in order to take on themselves the (possibly huge) plasma heat load. This can of course severely damage them, but it avoids at the same time a much more dangerous impact on the unprotected wall, preventing thus in-vessel LOCAs or complicated remote maintenance of the blanket modules (the substitution of a limiter being much simpler with this respect). It is however still to be demonstrated whether these limiters are indeed able to protect the FW in presence of all possible unplanned transients – this crucial open point being currently under investigation.

For the divertor, DEMO baseline relies on an ITER-like LSN configuration. Main deviation from the ITER concept are due to the introduction of divertor sweeping as emergency countermeasure, which is introduced in order to reduce even further the eventuality of a plasma-wall contact (due to a fast plasma termination) in case of divertor reattachment.

Also, the adoption of ELM-free scenarios in DEMO may lead to significant design changes in the machine, but this cannot be deeply investigated also in view of the present scarce understanding of those regimes, thus limiting the possibility of robustly extrapolating them to DEMO.

In summary, the main lesson learned in this first DEMO design phase is in fact that transients (ELMs, disruptions and divertor reattachment) play a much more important role than steady-state to drive the design and limit the reactor design space.

CRediT authorship contribution statement

F. Maviglia: Investigation, Formal analysis, Supervision. **M. Siccinio:** Writing - original draft, Investigation, Writing - review & editing. **C. Bachmann:** Investigation. **W. Biel:** Investigation, Supervision. **M. Cavedon:** Investigation. **E. Fable:** Investigation. **G. Federici:** Supervision. **M. Firdaouss:** Investigation. **J. Gerardin:** Investigation. **V. Hauer:** Investigation. **I. Ivanova-Stanik:** Investigation. **F. Janky:** Investigation.

R. Kembleton: Supervision. **F. Militello:** Supervision. **F. Subba:** Investigation. **S. Varoutis:** Investigation. **C. Vorpahl:** Supervision.

Declaration of Competing Interest

The authors declare that they have no known competing financial interests or personal relationships that could have appeared to influence the work reported in this paper.

Acknowledgments

This work has been carried out within the framework of the EUROfusion Consortium and has received funding from the Euratom Research and Training Programme 2014–2018 and 2019–2020 under grant agreement No 633053. The views and opinions expressed herein do not necessarily reflect those of the European Commission.

References

[1] European Research Roadmap to the Realisation of Fusion Energy (https://www.eurofusion.org/fileadmin/user_upload/EUROfusion/Documents/2018_Research_roadmap_long_version_01.pdf).
[2] G. Federici, et al., Nucl. Fusion 59 (2019), 066013.
[3] Mitteau R. et al., 2010 Fus. Eng. Design 85(10–12), 2049.
[4] F. Maviglia, et al., Fus. Eng. Design 136 (2018) 410.
[5] Bachmann C. et al., 2019 Fus. Eng. and Design 146, Part A, 178.
[6] F. Maviglia, et al., Fus. Eng. Design 158 (2020), 111713.
[7] Z. Vizvary, et al., Fus. Eng. Design 158 (2020), 111676.
[8] T.R. Barrett, et al., Nucl. Fusion 59 (2019), 056019.
[9] H. Reimerdes, et al., Nucl. Fusion 60 (2020), 066030.
[10] Militello F. et al., this conference.
[11] F. Maviglia, et al., Fus. Eng. Des. 109 (2016) 1067.
[12] M. Kovari, et al., Fus. Eng. Des. 89 (2014) 3054.
[13] M. Kovari, et al., Fus. Eng. and Des. 104 (2016) 9.
[14] M. Siccinio, et al., Fus. Eng. Des. 156 (2020), 111603.
[15] R. Aymar, et al., Plasma Phys. Control. Fusion 44 (2002) 519.
[16] B.J. Green, ITER International Team and Participant Teams, Plasma Phys. Control. Fusion 45 (2003) 687.
[17] F. Wagner, et al., Phys. Rev. Lett. 49 (1982) 1408.
[18] N.A. Uckan, ITER Physics Design Guidelines, ITERTN-PH-8-6 (1989).
[19] Moro F., 2018 Fus. Eng. Des. 136, Part B, 1260.
[20] P. Pereslavtsev, et al., Fus. Eng. Des 124 (2017) 910.
[21] F.A. Hernández, et al., Fus. Sci. Technol. 75 (2019) 352.
[22] R. Wenninger, et al., Nucl. Fusion 57 (2017), 046002.
[23] A. Loarte, et al., Nucl. Fusion 47 (2007) S203.
[24] G.V. Pereverzev, IPP Report 5/42 (1991).
[25] G.V. Pereverzev, P.N. Yushmanov, IPP Report 5/98 (2002).
[26] E. Fable, et al., Plasma Phys. Control. Fusion 55 (2013), 124028.
[27] F. Subba, et al., Plasma Phys. Control. Fusion 60 (2018), 035013.
[28] Subba F. et al., this conference.
[29] M. Carr, A. Meakins, cherab/core: Release v1.1.0, Zenodo (2019).
[30] M. Carr, A. Meakins, A. Baciero, C. Giroud, CHERAB's documentation, Available: https://cherab.github.io/documentation/index.html, 2018.
[31] J.H. You, et al., Nucl. Mater. Energy 9 (2016) 171.
[32] T. Eich, et al., Phys. Rev. Lett. 107 (2011), 215001.
[33] T. Eich, et al., Nucl. Fusion 53 (2013), 093031.
[34] D. Carralero, et al., Nucl. Fusion 57 (2017), 056044.
[35] R. Mitteau, P. Stangeby, H. Labidi, R. Bruno, R. Raffray, J. Nucl. Mater. 463411-4, in: Proc. of the 21st Int. Conf. on Plasma-Surface Interactions in Controlled Fusion Devices Kanazawa (Japan, 26–30 May 2014) (2015).
[36] Shimada M. et al., Heat and Nuclear Load Specifications for ITER.
[37] R. De Luca, et al., Fus. Eng. Des. 158 (2020), 111721.
[38] J. Gerardin, et al., Nucl. Mater. Energy 20 (2019), 100568.
[39] F. Maviglia, et al., Fus. Eng. Des. 124 (2017) 385.
[40] M. Firdaouss, V. Riccardo, V. Martin, G. Arnoux, C. Reux, J. Nucl. Mater. 438S536-9, in: Proc. of the 20th Int. Conf. on Plasma-Surface Interactions in Controlled Fusion Devices, (2013).
[41] R. Albanese, R. Ambrosino, M. Mattei, Fus. Eng. Des. 96 (2015) 664.
[42] Albanese R. et al., 2019 Fus. Eng. and Des.146, Part B, 1468.
[43] J. Varje et al., 2019 Fus. Eng. Des. 146(Part B), 1615.
[44] G. Bustos Ramirez, et al., 2020 Final Report https://idm.euro-fusion.org/?uid=2NT4R6 (unpublished).
[45] T. Kurki-Suonio et al., https://idm.euro-fusion.org/?uid=2MCWAE (unpublished).
[46] M. Beckers, et al., Nucl. Mater. Energy 12 (2017) 1163.
[47] M.Z. Tokar, Nucl. Fusion 58 (2018), 016016.
[48] M.Z. Tokar, Nucl. Fusion 59 (2019), 076002.
[49] W. Biel, et al., Fus. Eng. Des. 96–97 (2015) 8.
[50] W. Biel, et al., Fus. Eng. Des. 146 (2019) 465–472.
[51] J. Horacek, et al., Plasma Phys. Control. Fusion 58 (2016), 074005.
[52] M. Kočan, et al., Nucl. Fusion 55 (2015), 033019.
[53] C. Silva, J.E. Contributors, Nucl. Fusion 54 (2014), 083022.
[54] F. Felici, et al., Nucl. Fusion 51 (2011), 083052.
[55] https://idm.euro-fusion.org/?uid=2NEGGD (unpublished).
[56] J. Keep, et al., Fus. Eng. and Des. 124 (2017) 420.
[57] S. Pestchanyi, F. Maviglia, Fus. Sci. Technol. 75 (2109), 647.
[58] F. Maviglia et al., Fus. Eng. Des. 146(Part A) (2019), 967.
[59] C. Bachmann, et al., Fus. Eng. Des. 156 (2020), 111595.
[60] L. Aho-Mantila, et al., this conference.
[61] L. Xiang, et al., this conference.
[62] R. Wenninger, et al., Nucl. Fusion 55 (2015), 063003.
[63] R. Pitts, et al., Nucl. Mater. Energy 20 (2019), 100696.
[64] S. Varoutis, et al., Fus. Eng. Des. 12 (2017) 668.
[65] T.h. Eich, et al., Nucl. Fusion 58 (2018), 034001.
[66] E. Kaveeva, et al., Nucl. Fusion 58 (2018), 126018.
[67] W. Dekeyser, et al., this conference.
[68] E. Kaveeva, et al., Nucl. Fusion 60 (2020), 046019.
[69] E. Sytova, PhD thesis, https://pure.mpg.de/rest/items/item_3238763_2/component/file_3238774/content.
[70] A.R. Raffray, G. Federici, J. Nucl. Mater. 244 (1997) 85.
[71] M. Siccinio, et al., Nucl. Fusion 59 (2019) 10602.
[72] M.L. Reinke, Nucl. Fusion 57 (2017), 034004.
[73] R.J. Goldston, M.L. Reinke, J.A. Schwartz, Plasma Phys. Control. Fusion 59 (2017), 055015.
[74] M. Siccinio, et al., Nucl. Fusion 58 (2018), 016032.
[75] M. Siccinio, et al., Plasma Phys. Control. Fusion 58 (2016), 125011.
[76] T.h. Eich, et al., Nucl. Mater. Energy 12 (2017) 84.
[77] A. Hassanein, I. Konkashbaev, J. Nucl. Mater 233–237 (Part 1) (1996) 713.
[78] K.H. Burrell, et al., Plasma Phys. Control. Fusion 44 (2002) A253.
[79] D. Whyte, et al., Nucl. Fusion 50 (2010), 105005.
[80] Y. Camenen, et al., Nucl. Fusion 57 (2017), 086002.
[81] S.Y. Medvedev, et al., Nucl. Fusion 55 (2015), 063013.
[82] M. Austin, et al., Phys. Rev. Lett. 122 (2019), 115001.
[83] L. Gil, et al., Nucl. Fusion 60 (2020), 054003.
[84] M. Bernert, this conference.